BEATS_eu
@BEATSeu1

BEATS

BEAmline for Tomography at SESAME

BEATS: The Tomography Beam Line at SESAME

Gianluca Iori

BEATS beamline scientist, SESAME, Jordan

gianluca.iori@sesame.org.jo

www.beats-sesame.eu

Funded by the EU's H2020 framework programme under grant agreement n°822535

ALBA The Cyprus Institute DESY. Elettra Sincrotrone Trieste ESRF INFN LNF PAUL SCHERRER INSTITUT PSI SESAME SOLARIS NATIONAL SYNCHROTRON RADIATION CENTRE

BEAmline for Tomography at SESAME Project

BEATS, the BEAmline for Tomography at SESAME is an H2020 European project to build a beamline for tomography at the SESAME synchrotron in Jordan.

More about the project →

Funded by the EU's H2020 framework programme under grant agreement n°822535

Outlook

Part 1: The BEATS beamline of SESAME

- X-Ray Computed Tomography (CT) with a synchrotron source
- Laboratory VS synchrotron X-Ray CT
- Design and status of BEATS installation

Part 2: Scientific opportunities @ BEATS

- Archaeology and cultural heritage
- Health, biology and food
- Agriculture and environment
- Material science and engineering

BEAmline for Tomography at SESAME

Funded by the EU's H2020 framework programme under grant agreement n°822535

X-ray computed tomography

BEATS

BEAmline for Tomography at SESAME

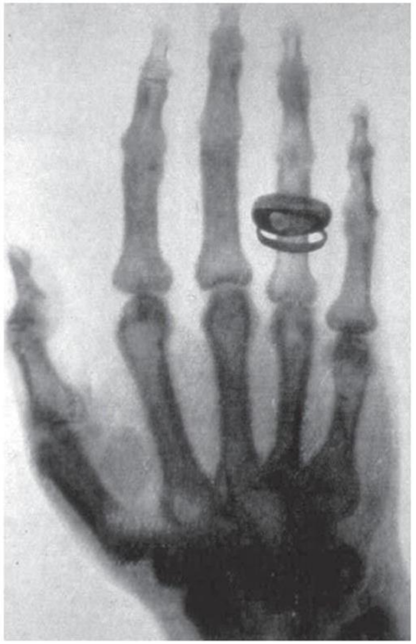

First Radiograph (1895)

First Computed Tomography scan
EMI Scanner (1971)

Nobel prize for CT in 1979
Hounsfield & Cormack

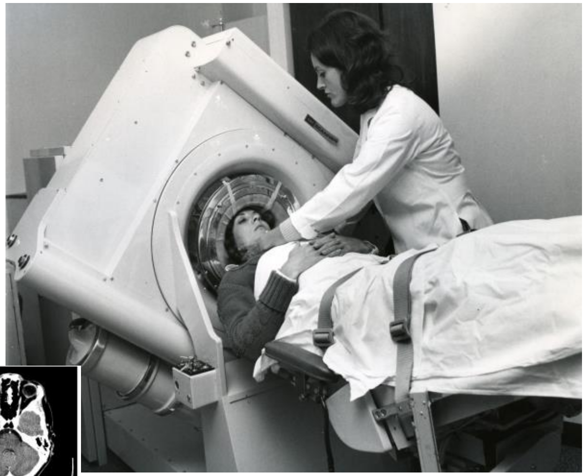

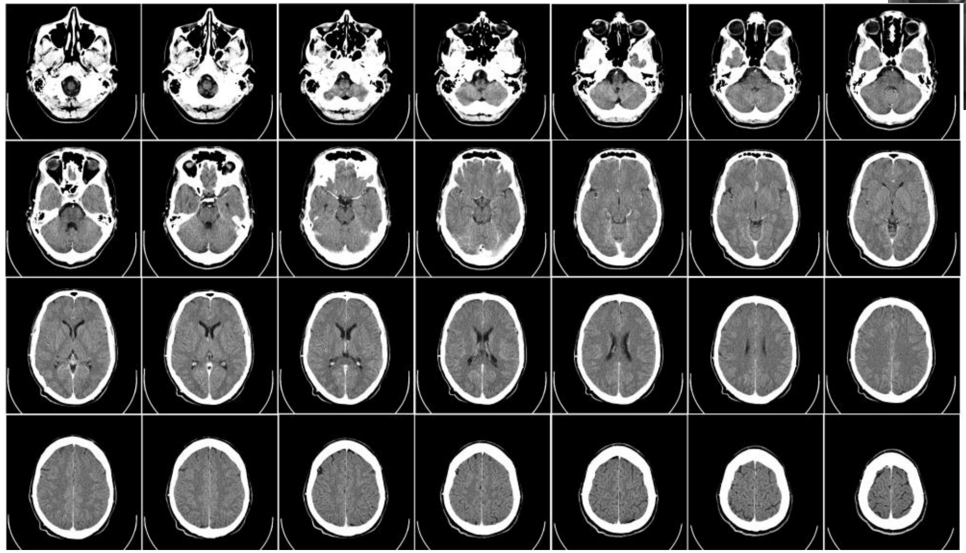

Funded by the EU's H2020 framework programme under grant agreement n°822535

BEATS

BEAmline for Tomography at SESAME

X-ray computed tomography

First Computed Tomography scan
EMI Scanner (1971)

Nobel prize for CT in 1979
Hounsfield & Cormack

https://www.psi.ch/en/sls/tomcat/endstations

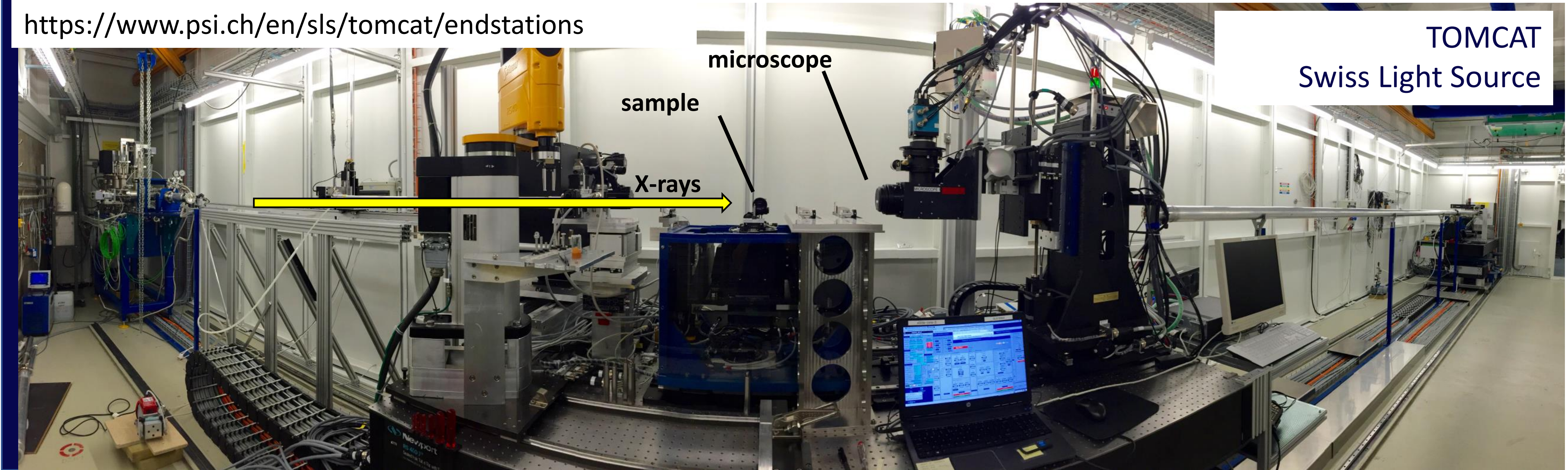

TOMCAT
Swiss Light Source

X-ray computed tomography

BEATS

BEAmline for Tomography
at SESAME

https://www.psi.ch

First Computed Tomography scan
EMI Scanner (1971)

Nobel prize for CT in 1979
Hounsfield & Cormack

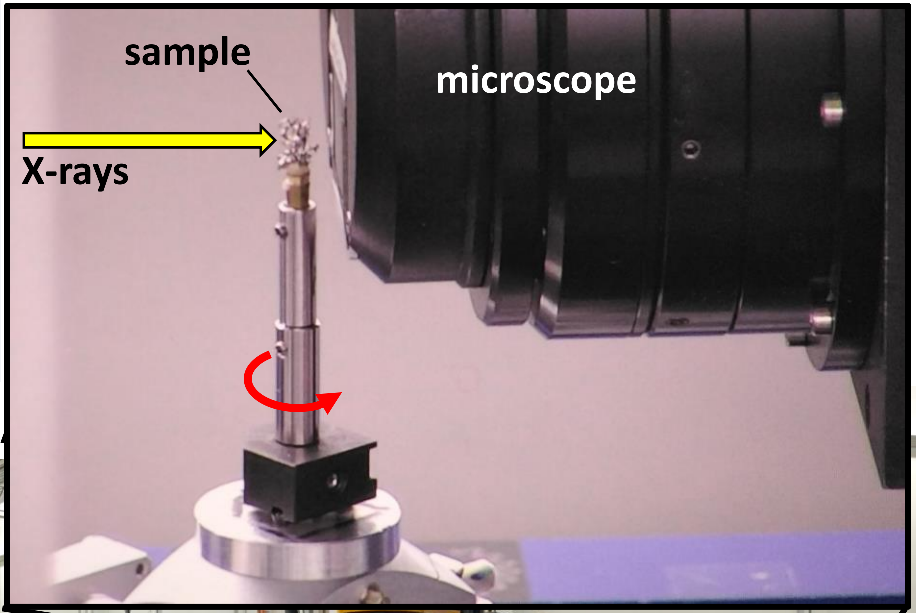

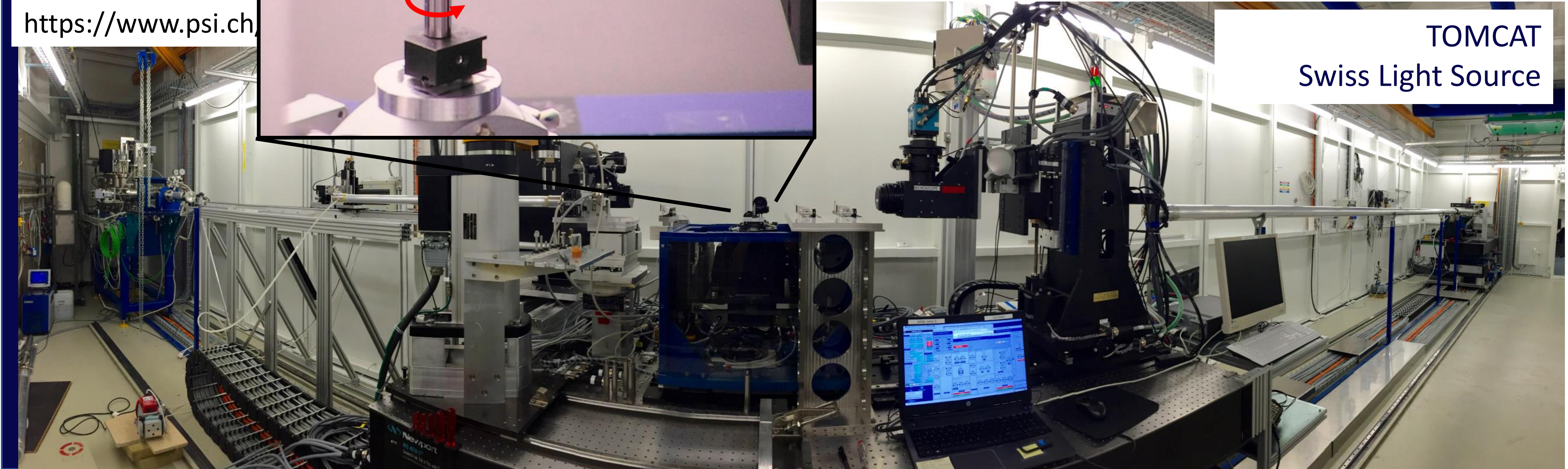

TOMCAT
Swiss Light Source

Laboratory XCT

- Wide spectrum of (**polychromatic**) X-ray energies, with bright peaks characteristic of the source target material
- **Cone-beam** geometry

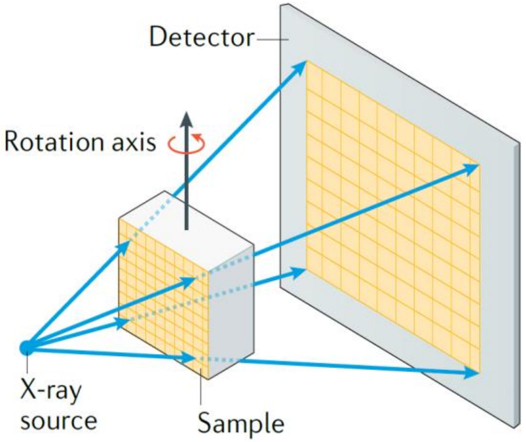

- Can illuminate **large objects** and exploit physical magnification
- **Typical scan times: hours to minutes**

Synchrotron XCT

- **Higher flux** by several orders of magnitude
- **Monochromatic X-ray beam** possible: improved sensitivity and limited artefacts
- High spatial coherence enables **phase contrast**
- **Parallel-beam geometry**

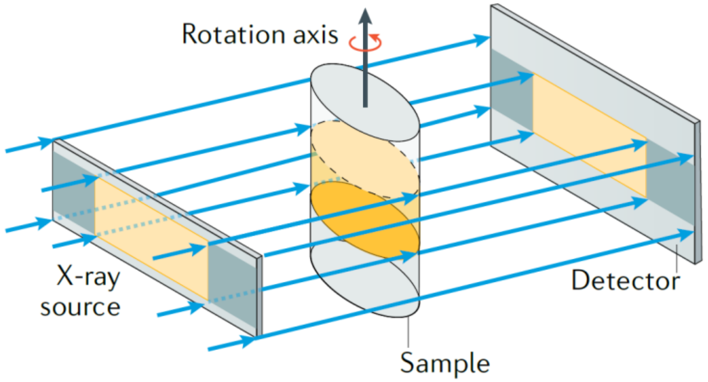

- (Generally) **higher resolution**
- (But) smaller field of view
- **Typical scan times: minutes to <seconds**
- **Time-resolved (4D) CT**

[Withers et al. 2021]

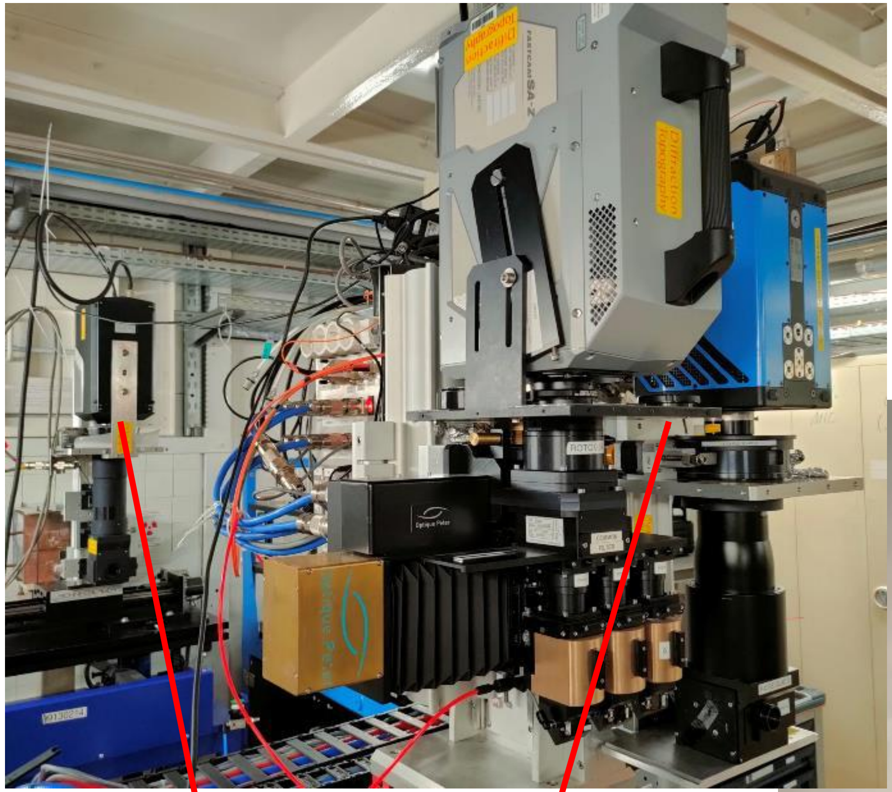

10 MHz

100 kHz

StructureOfMaterials

@SoM_esrf Follows you

The Structure of Materials Group @esrfsynchrotron provides world-class facilities for hard X-ray diffraction, scattering and microimaging experiments.

Grenoble, France esrf.eu/UsersAndScienc... Joined February 2016

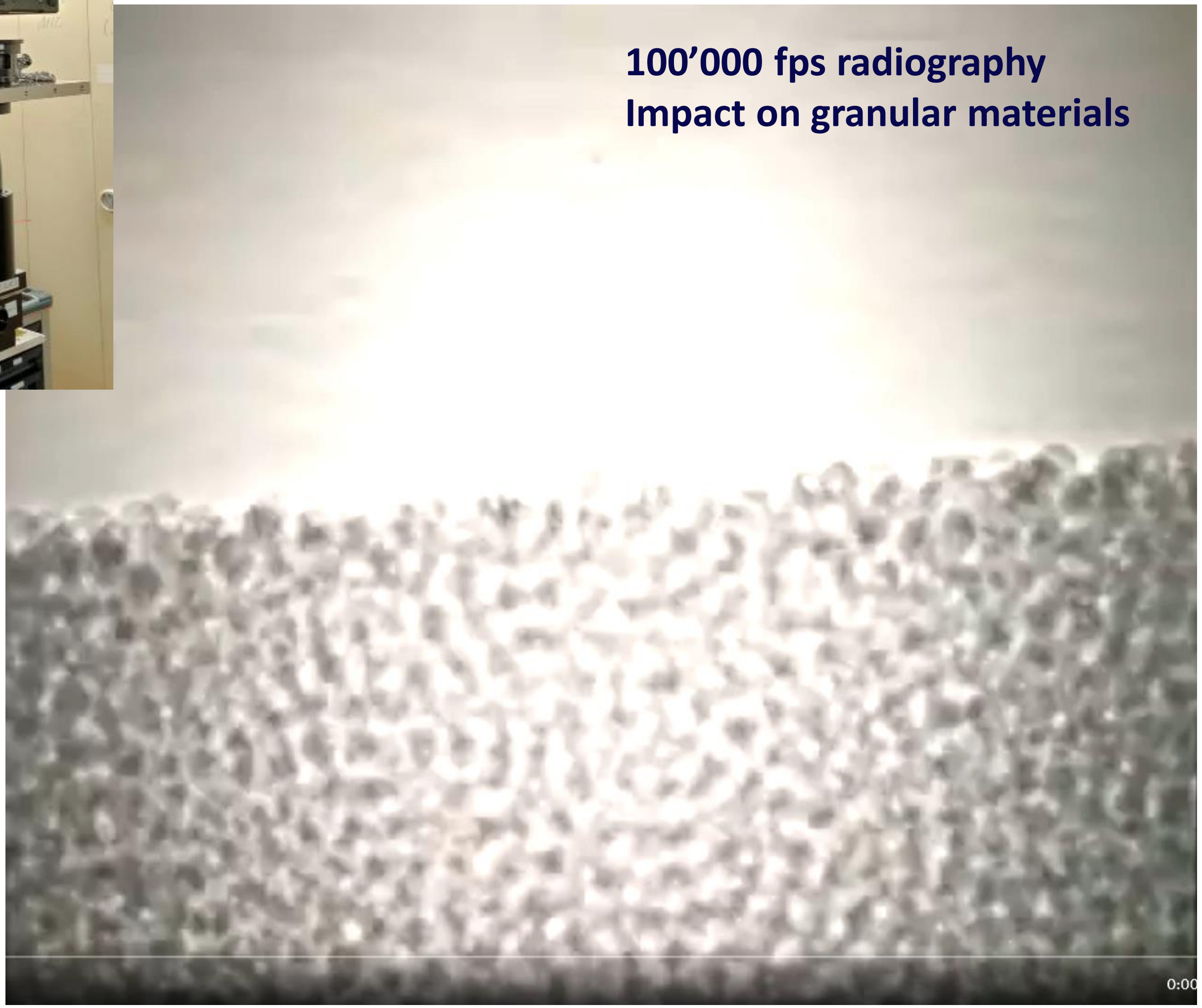

In-situ mechanical testing

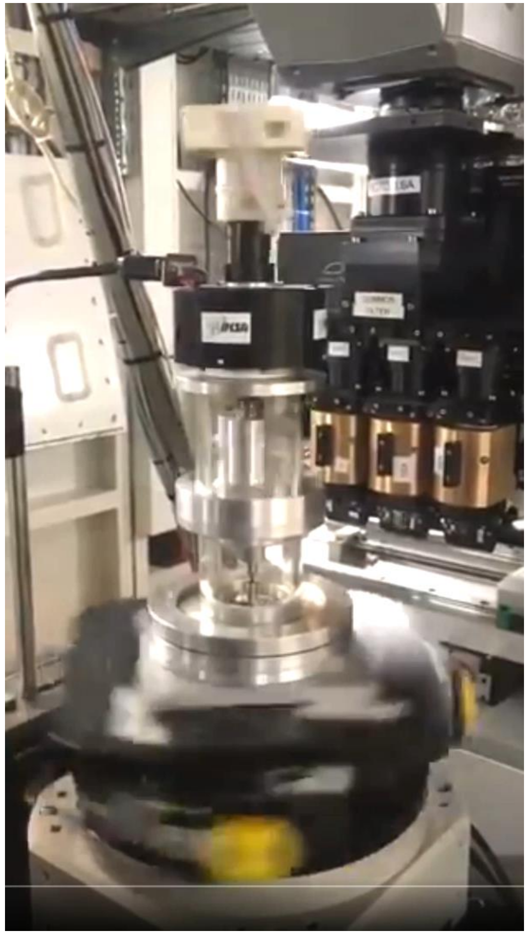

The BEATS beamline at a glance

Total Length	45 m
Energy range	8 – 100 keV
Divergence	1.8 mrad (H) × 0.4 mrad (V)
Detectors	0.5× – 10× optics; 5.5MP sCMOS camera
Available voxel size	13 – 0.65 µm
Beam size @ sample	72 mm (H) × 15 mm (V) (white beam)
Modalities	• Filtered white beam • Monochromatic (with DMM)

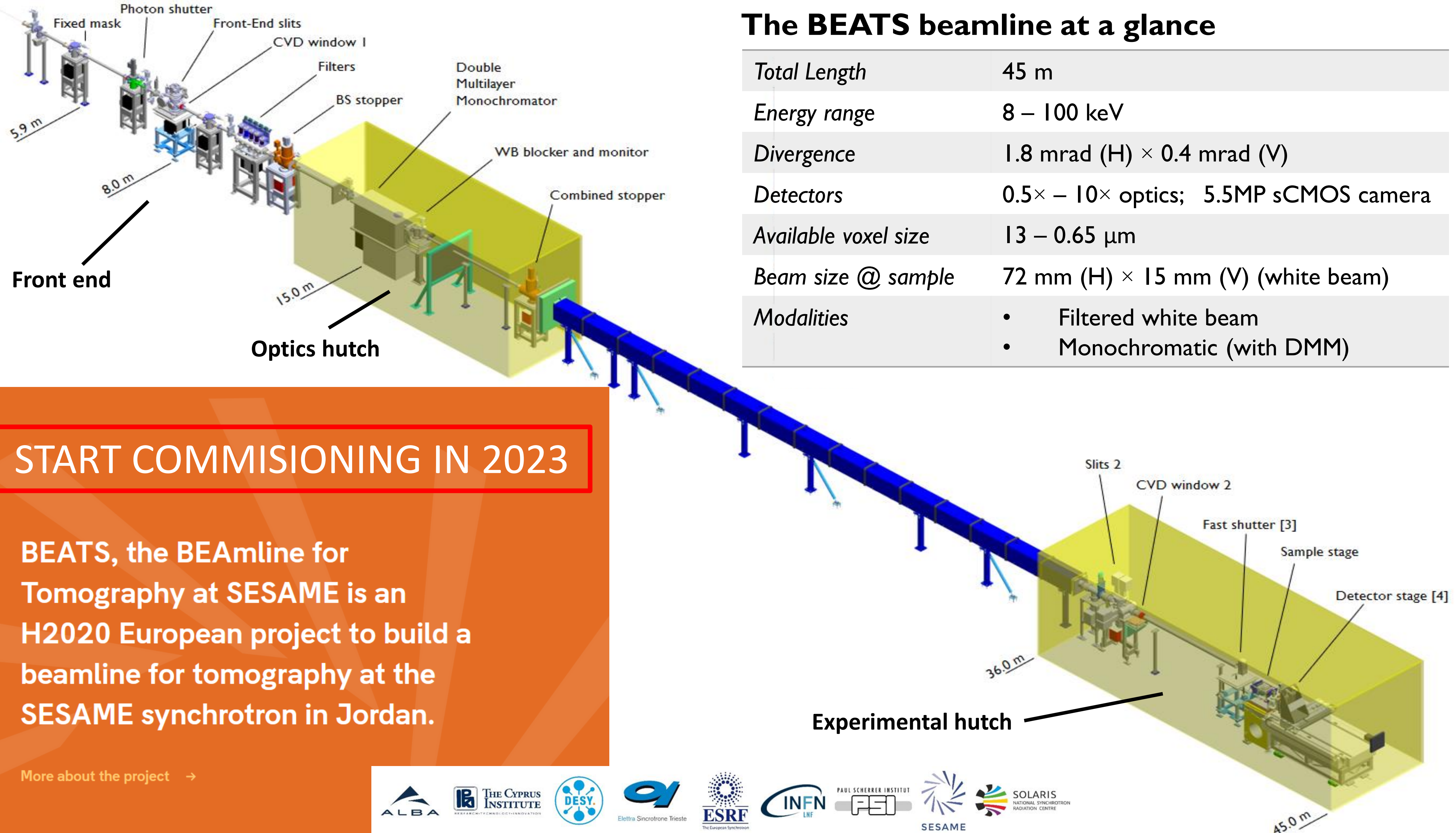

START COMMISIONING IN 2023

BEATS, the BEAmline for Tomography at SESAME is an H2020 European project to build a beamline for tomography at the SESAME synchrotron in Jordan.

More about the project →

BEATS layout

- **High-flux**; well above 20 keV to see through large, dense samples
- Filtered **white beam (high-flux)** VS **monochromatic beam (high-sensitivity)** (with DMM)

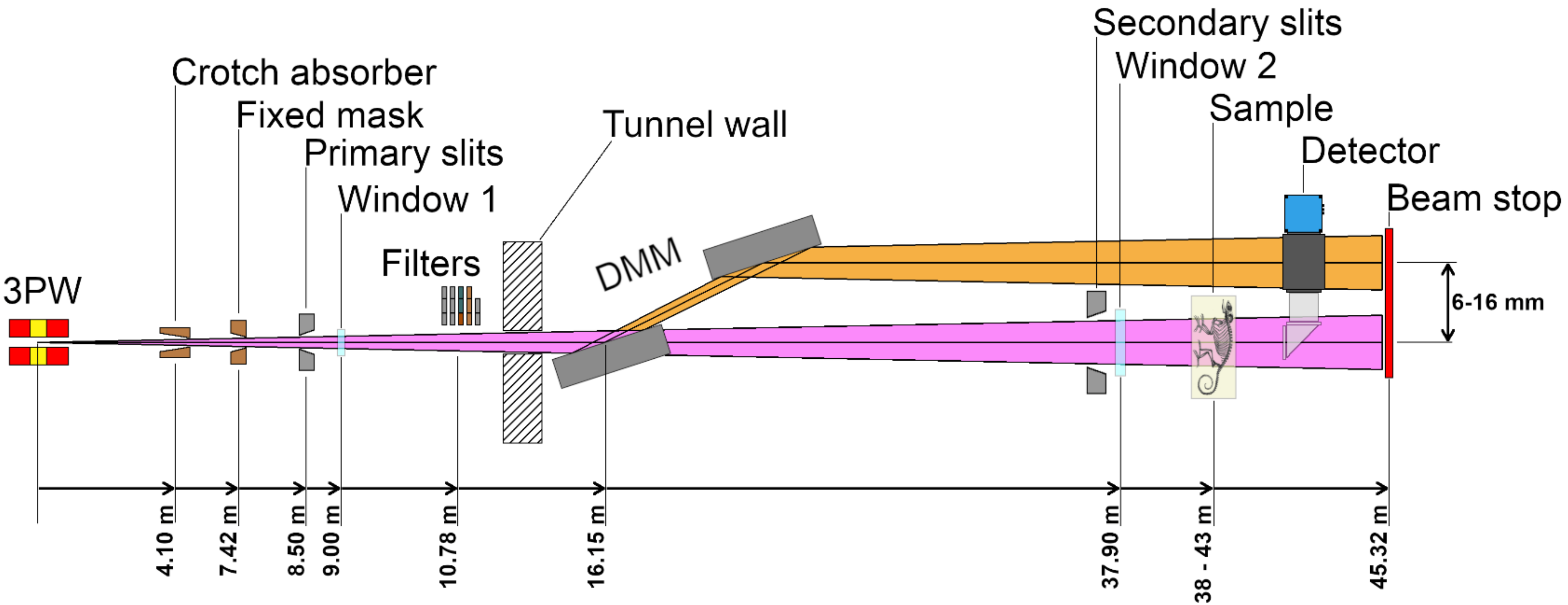

Maximize beamline length to improve spatial coherence and decrease image blur!

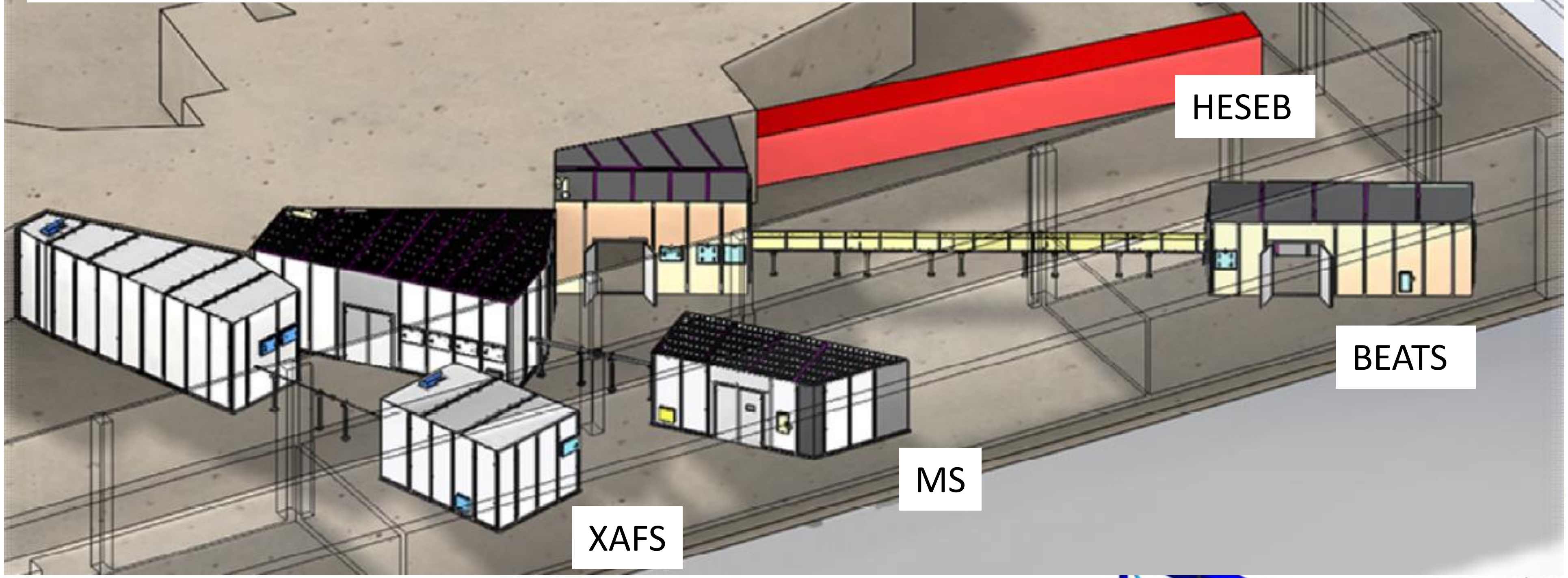

$$blur = \frac{SDD\ \sigma_x}{d}$$

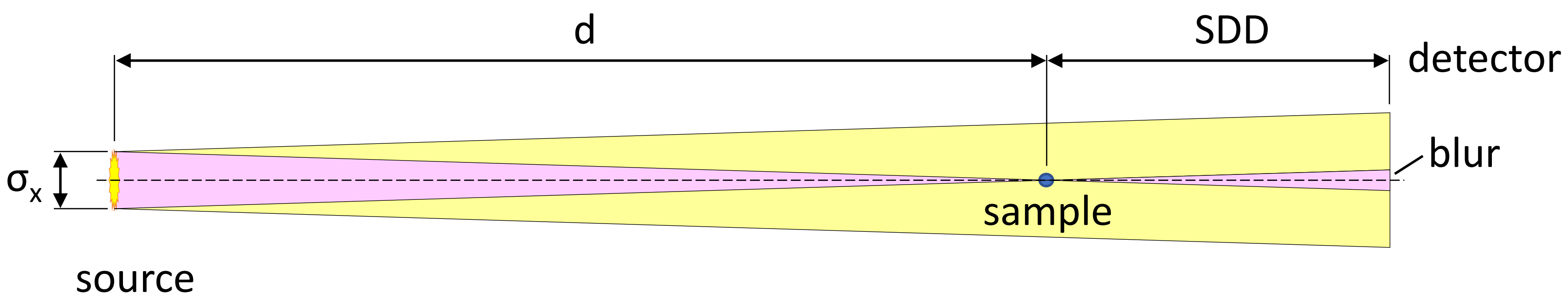

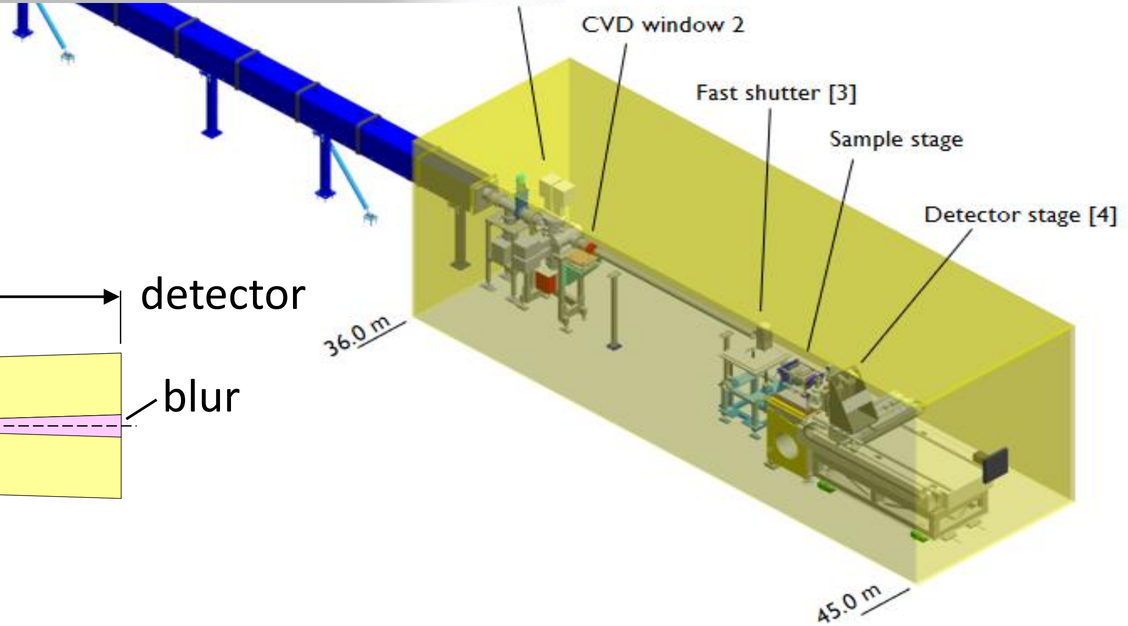

BEATS layout

- Coherence length and blur

Distance from source

$$l_{coh} = \frac{2\lambda d}{\sigma_x}$$

Source size

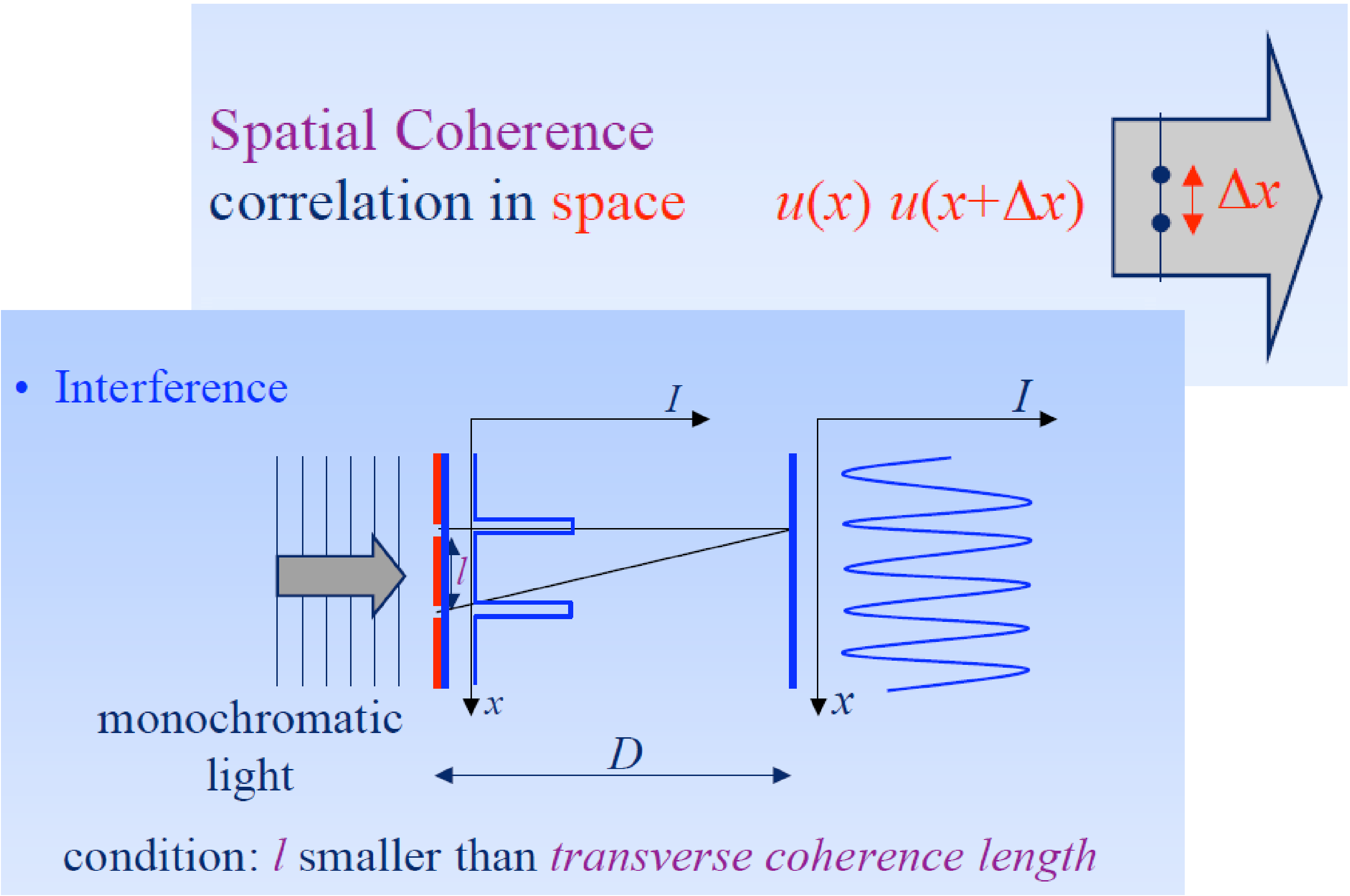

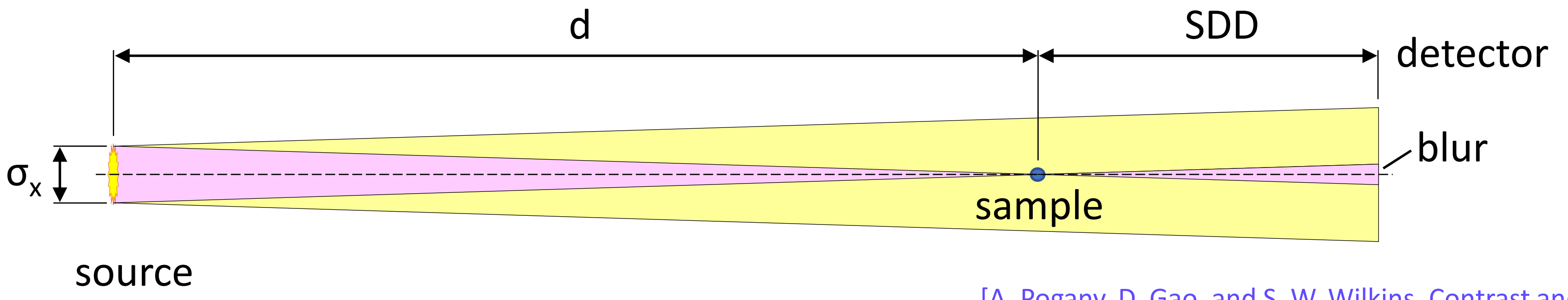

[A. Pogany, D. Gao, and S. W. Wilkins, Contrast and resolution in imaging with a microfocus x-ray source, 1997]
[P. Cloetens, Phase Contrast Imaging - Coherent Beams, School on X-ray Imaging Techniques at the ESRF, 2007]

BEATS layout

- Close Front-End slits (secondary source) for improved coherence

↓

<u>phase contrast</u>

- This reduces available flux and beam size!

Beamline	d [m]	σ_x [μm]	Transverse coherence length [μm]
ID19@ESRF	145	25	720.1
TOMCAT@SLS	34	140	30.2
SYRMEP@Elettra	23	197	14.5
TopoTomo@ANKA	33	500	8.2
BEATS - Primary slits OPEN	43	1978	2.7
BEATS - Primary slits: 1 mm (H)	34.6	1000	4.3
BEATS - Primary slits: 0.5 mm (H)	34.6	500	8.6

Table 9: transverse coherence length at 20 keV. Comparison of BEATS with other tomography beamlines.

BEATS X-Ray source

Three-pole wiggler

- Minimum gap: 11 mm
- Maximum field: 2.92 T
- Magnetic length: 0.41 m

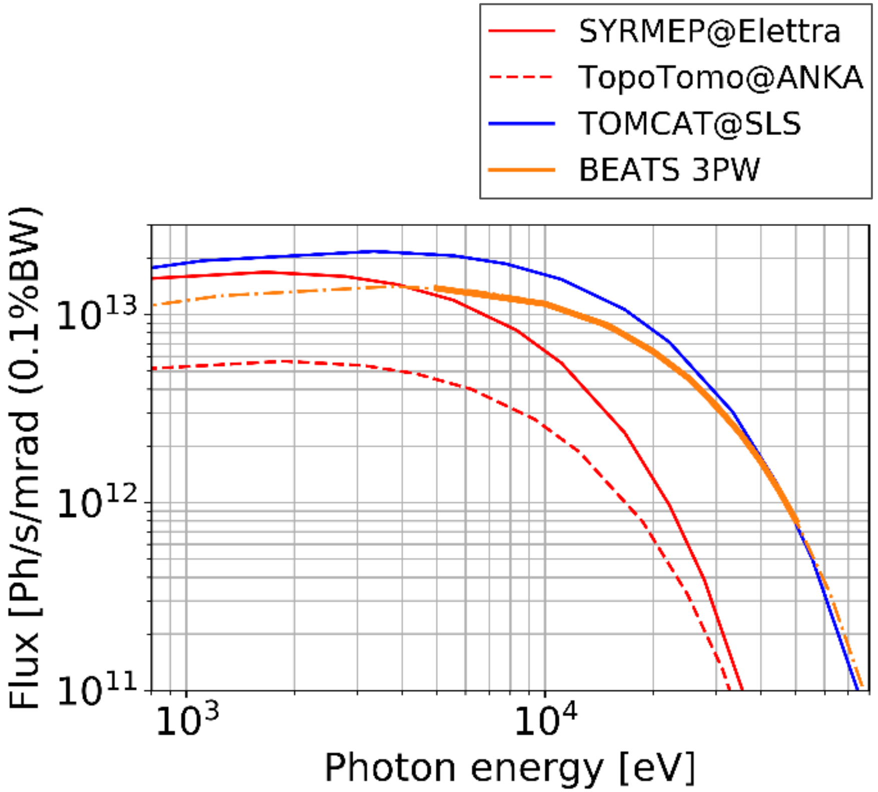

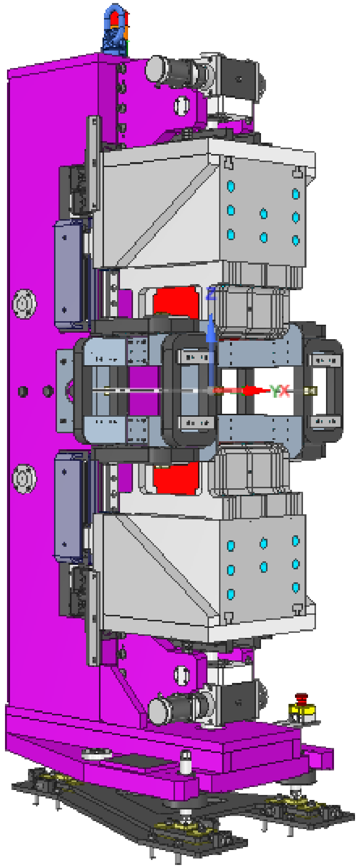

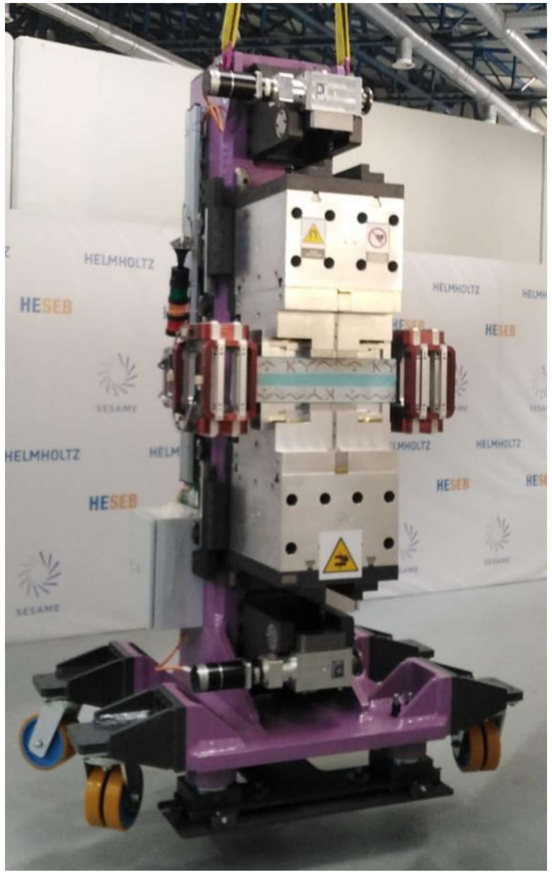

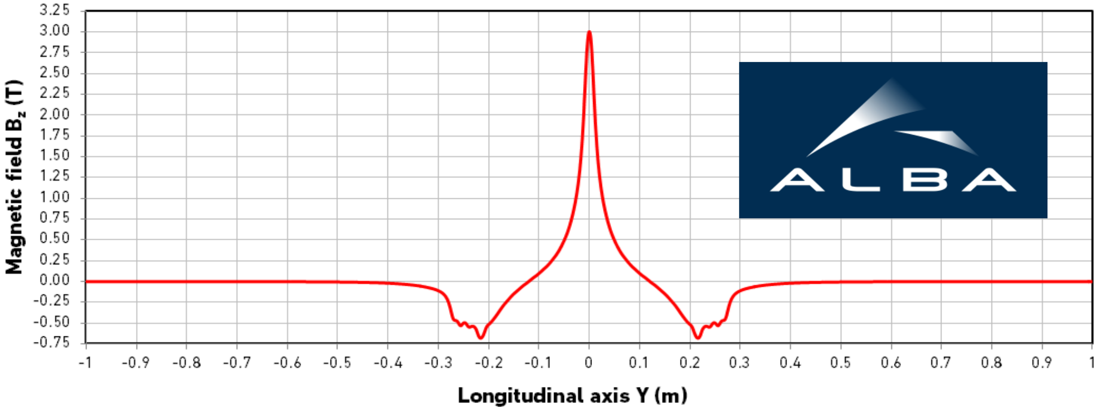

AUGUST-SEPTEMBER shutdown – ID and front-end installation

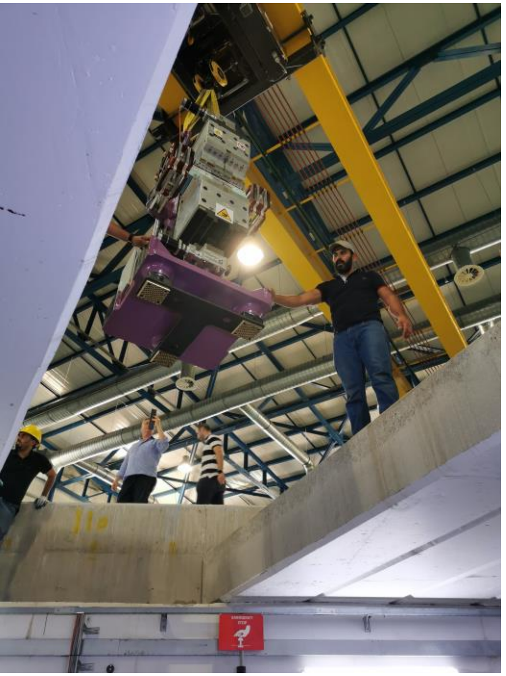

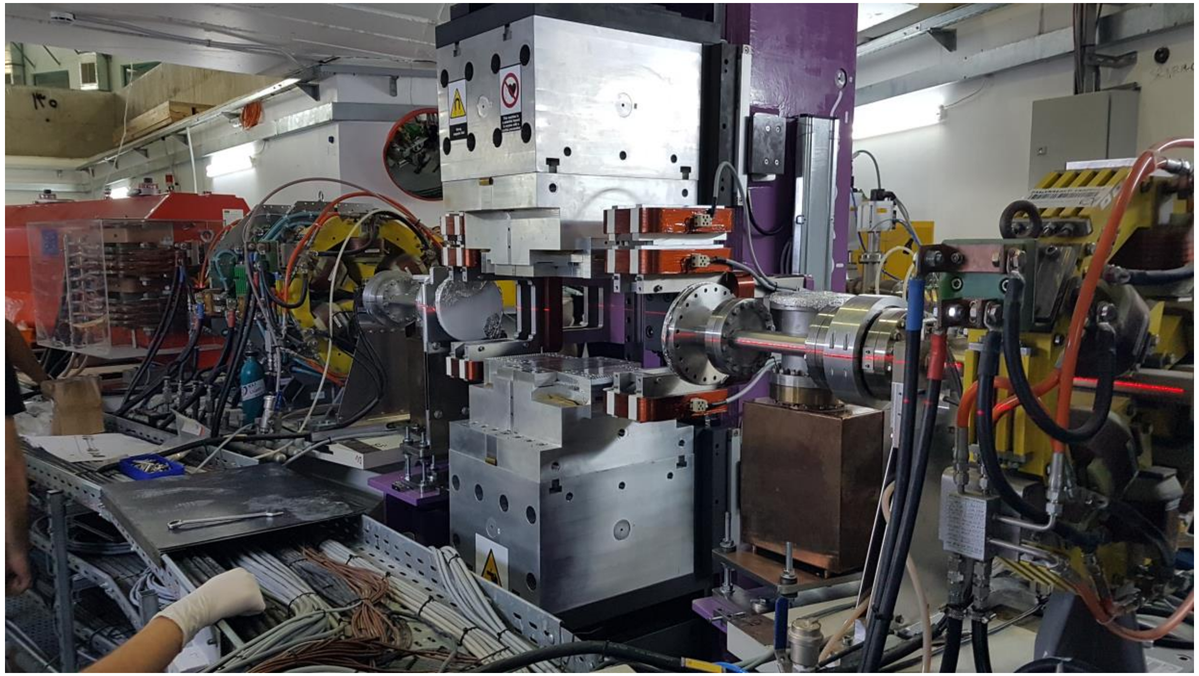

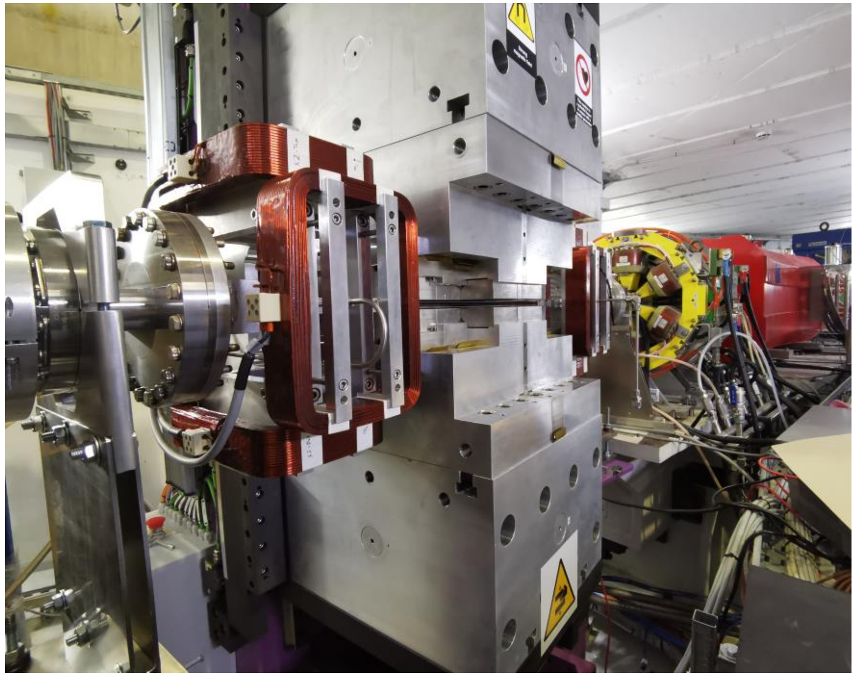

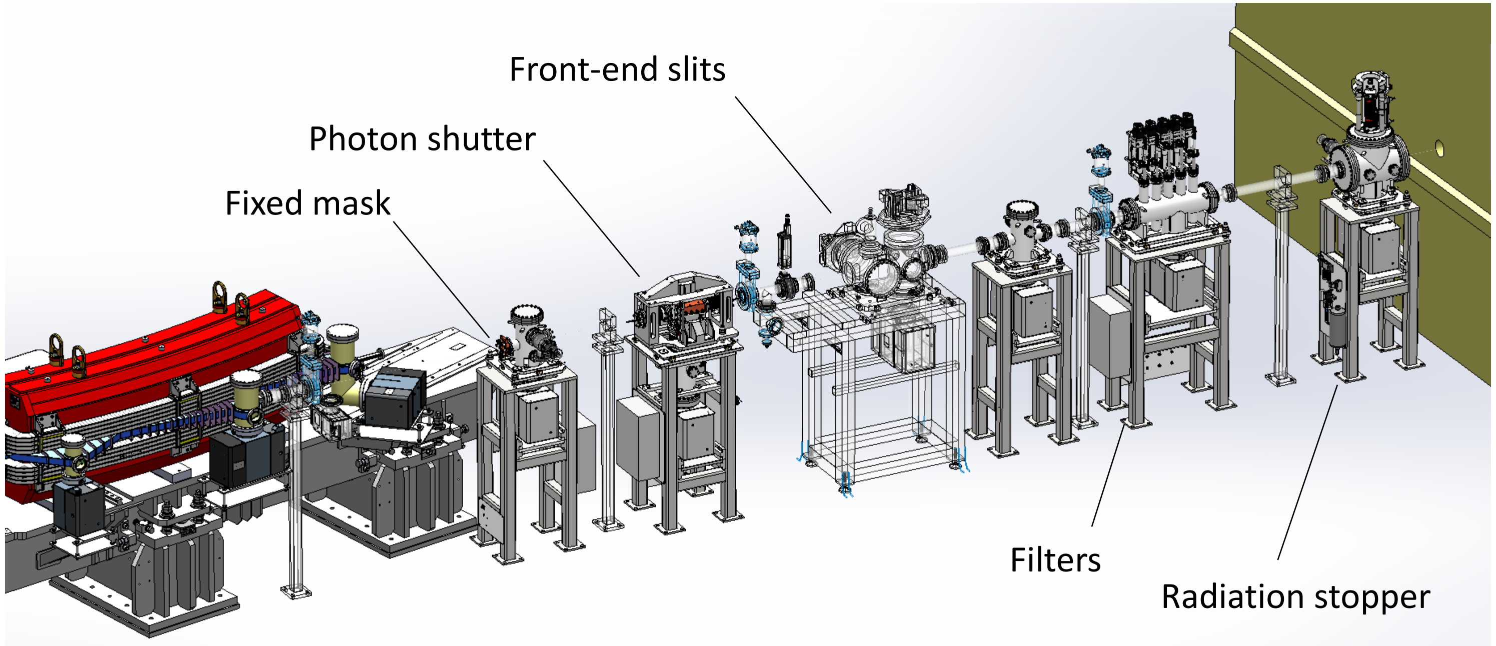

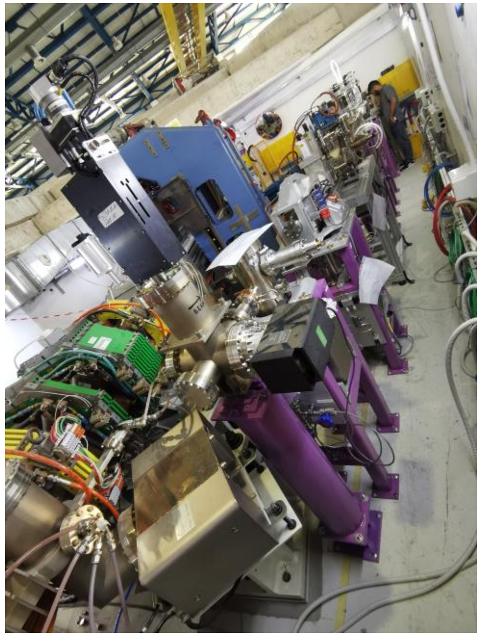

Beamline Optics:
Double Multilayer Monochromator (DMM)

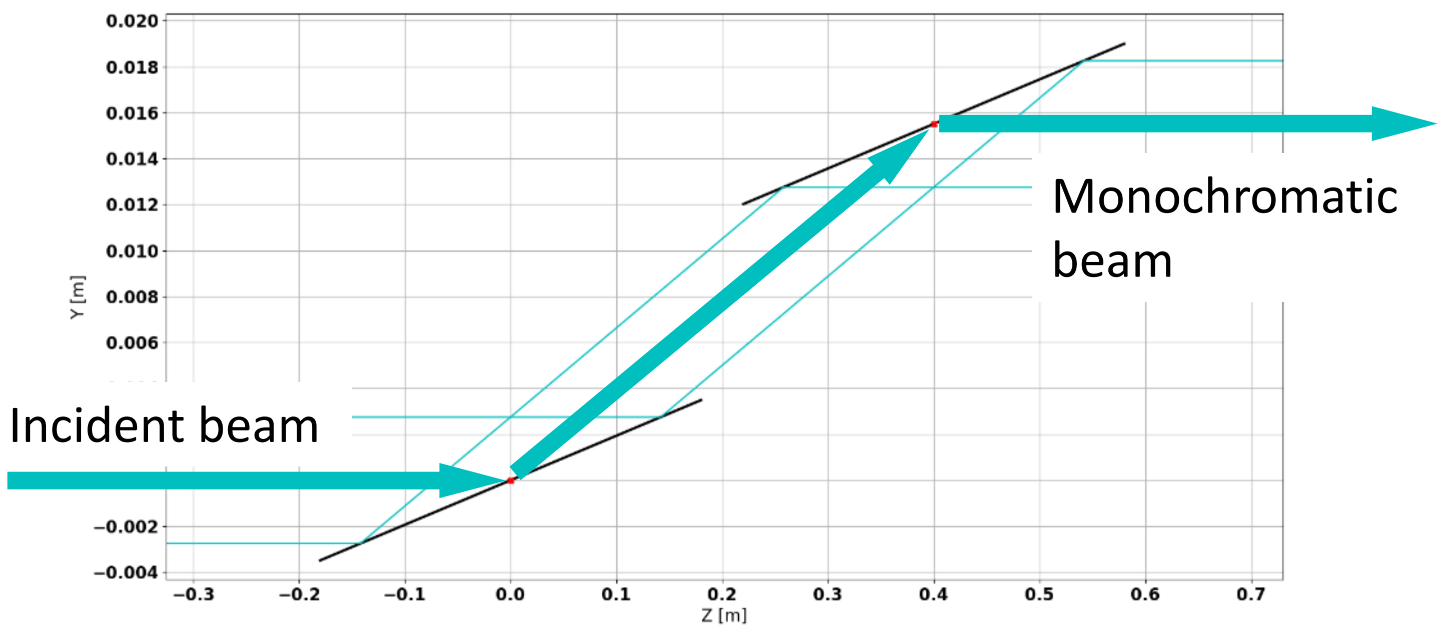

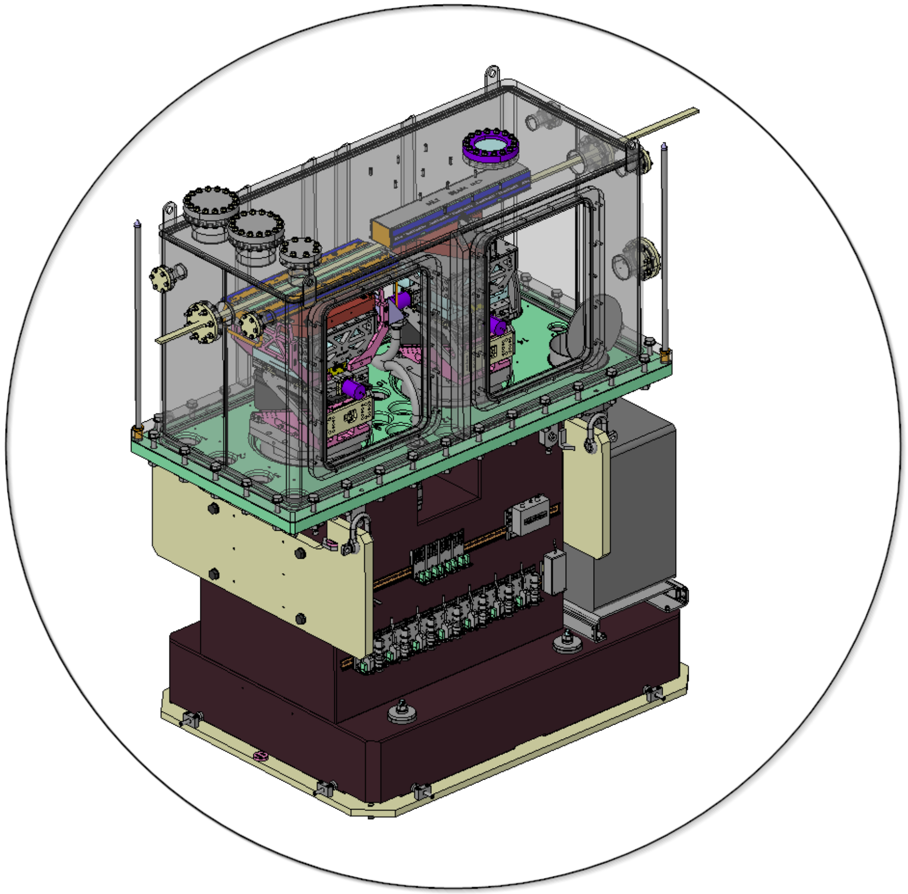

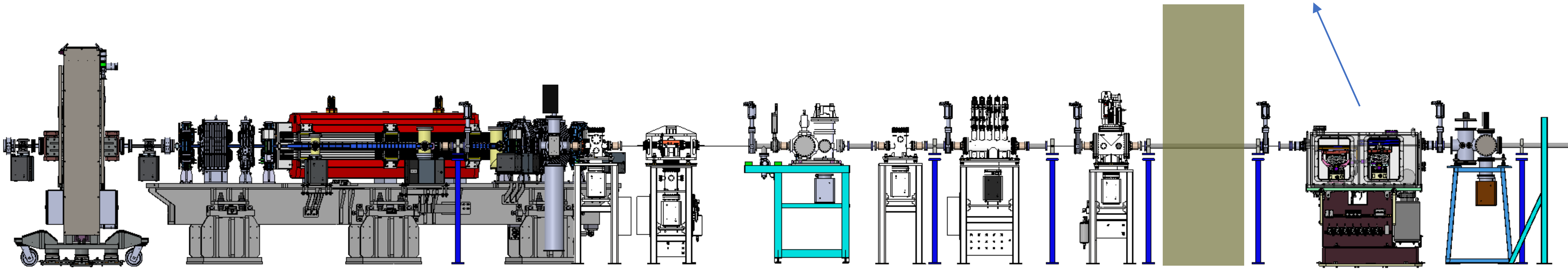

Double Multilayer Monochromator (DMM)

Multilayers

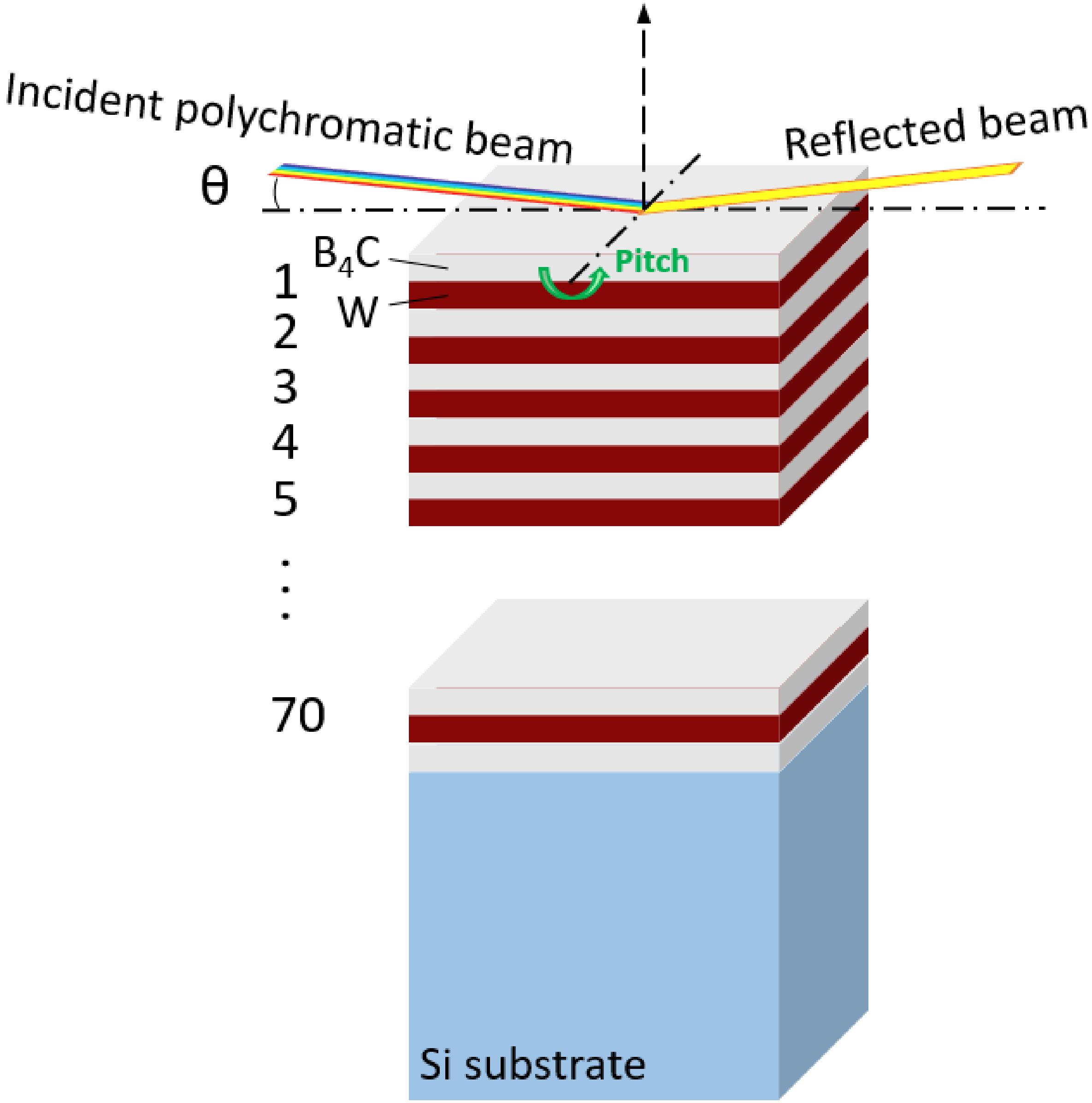

- Multilayers are produced by coating a Si substrate with periodic bi-layers of a high-Z and a low-Z material.
- The deposition process is called magnetron sputtering.
- Bragg's law for a multilayer:

$$\lambda = 2\, d \sin(\vartheta)$$

Bi-layer thickness

Double Multilayer Monochromator (DMM)

Multilayers

- Reflectivity as a function of photon energy for a Ru/B_4C multilayer for $\theta = 1.15°$ (BM5, ESRF)

- Limited number of scattering planes: less degree of monochromaticity and larger bandwidth than DCMs

ΔE/E	
DCM:	$10^{-4} \div 10^{-5}$
DMM:	10^{-2}

- Ru- and B_4C sublayers are equally thick: even harmonics suppressed

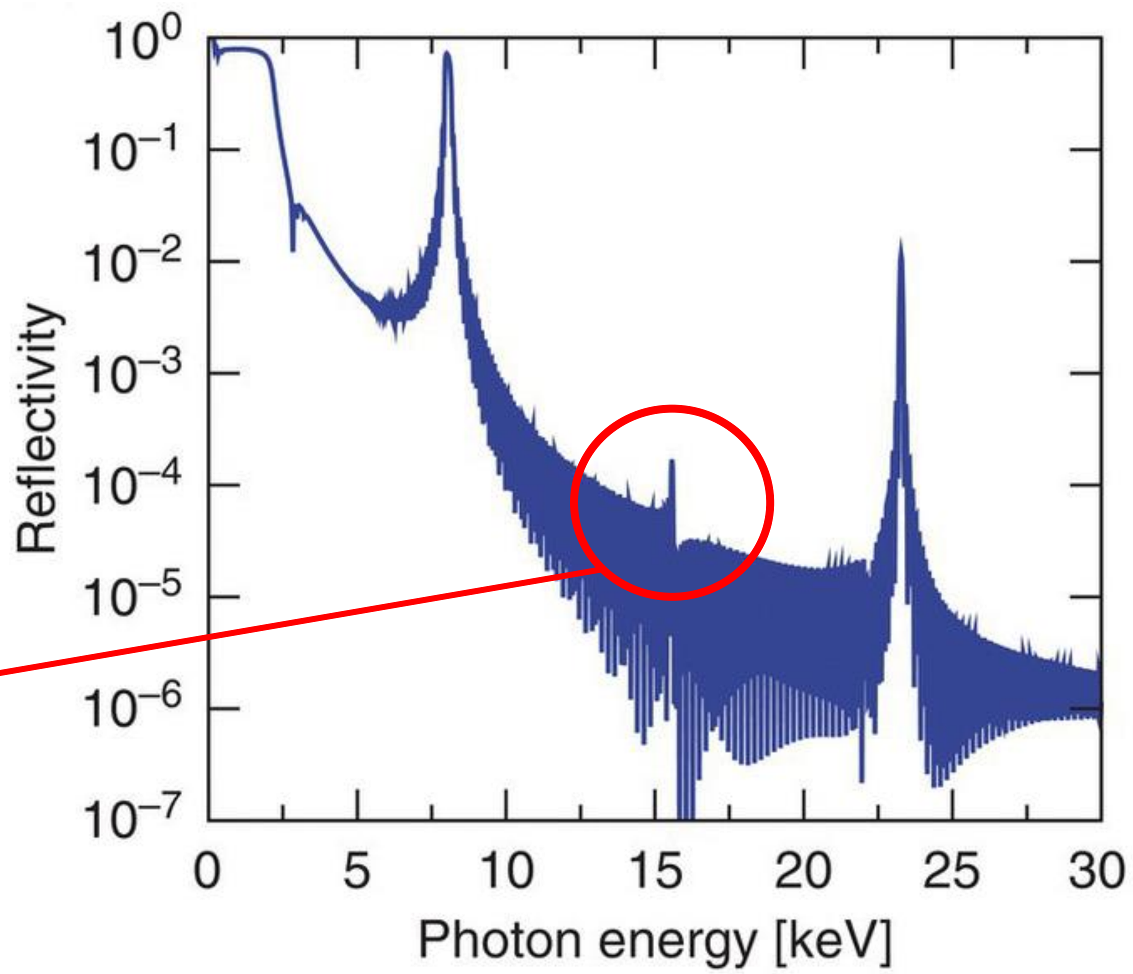

[An Introduction to Synchrotron Radiation: Techniques and Applications 2nd edition - Philip Willmott, 2018]

Double Multilayer Monochromator (DMM)

Substrates (BEATS)

Dimensions	500 mm × 65 mm × 60 mm
Coatings area	480 mm × 25 mm (2 stripes)
Surface roughness (RMS)	< 0.10 nm
Meridional slope error (RMS)	< 0.2 µrad

- Larger d implies smaller grazing angle and longer Si substrates than those of DCMs

Multilayers (BEATS)

	Stripe 1	Stripe 2
	$[W/B_4C]_{100}$	$[Ru/B_4C]_{65}$
Energies [keV]	20 – 50	8(10) – 22
d-spacing [nm]	3.0	4.0
Duty cycle γ	0.5	0.5
N. bilayers	100	65
dE/E [%]	~ 3.0	~ 3.1 %
Theta (Bragg angle) [deg]	0.22 – 0.75	0.40 – 1.10

Bi-layer thickness

$$\lambda = 2\,d\,\sin(\vartheta)$$

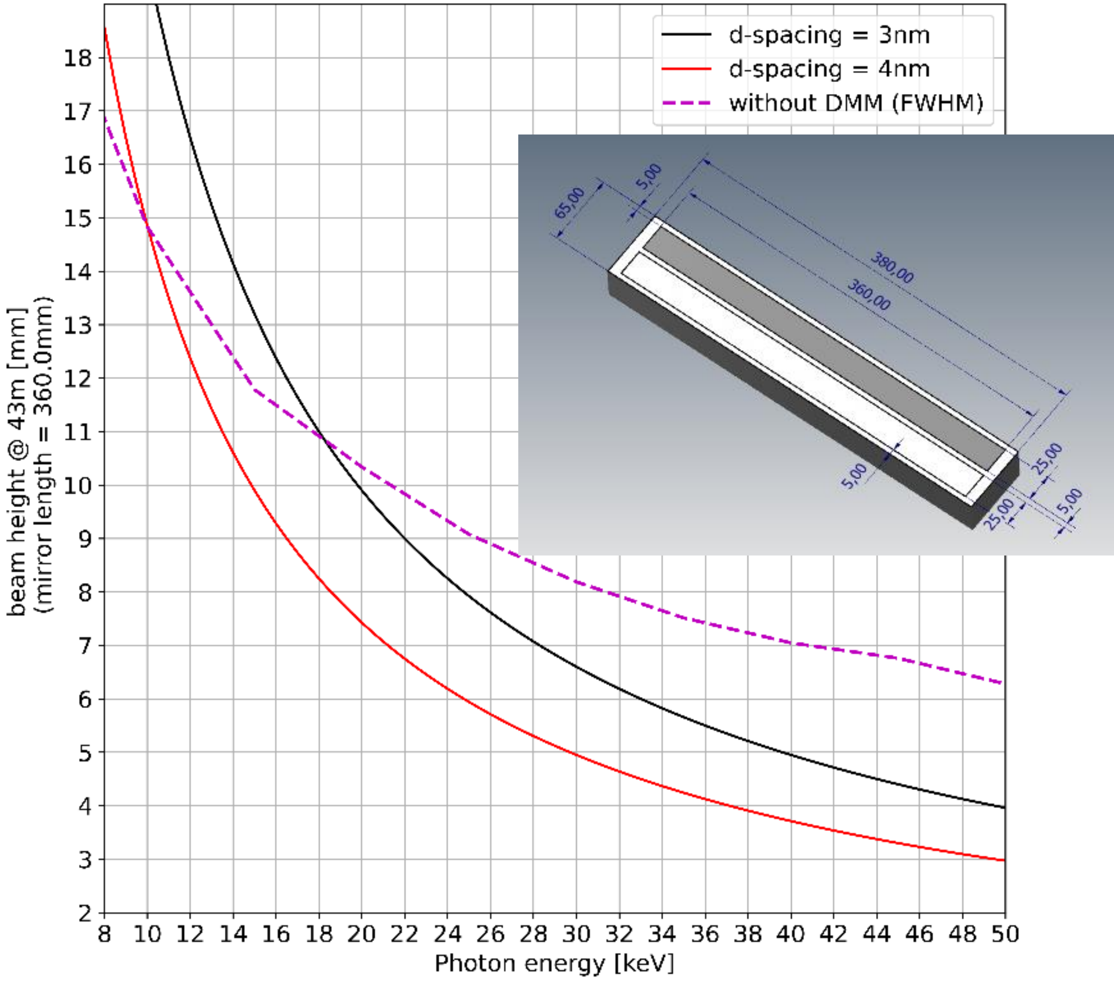

ESRF
The European Synchrotron
Multilayer laboratory

Double Multilayer Monochromator (DMM)

Substrates (BEATS)

Dimensions	500 mm × 65 mm × 60 mm
Coatings area	480 mm × 25 mm (2 stripes)
Surface roughness (RMS)	< 0.10 nm
Meridional slope error (RMS)	< 0.2 µrad

- $[W/B_4C]100$ DMM stripe @ 45 keV
- Meridional slope error: 0.1 – 0.5 µrad..

..The quality of the flat field deteriorates for mirror slope errors > 0.2 µrad!

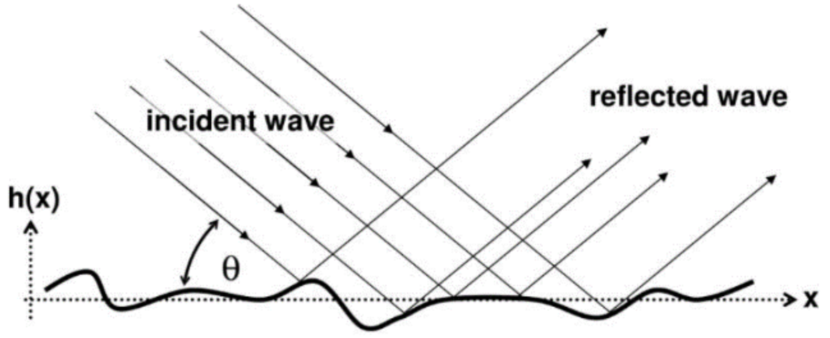

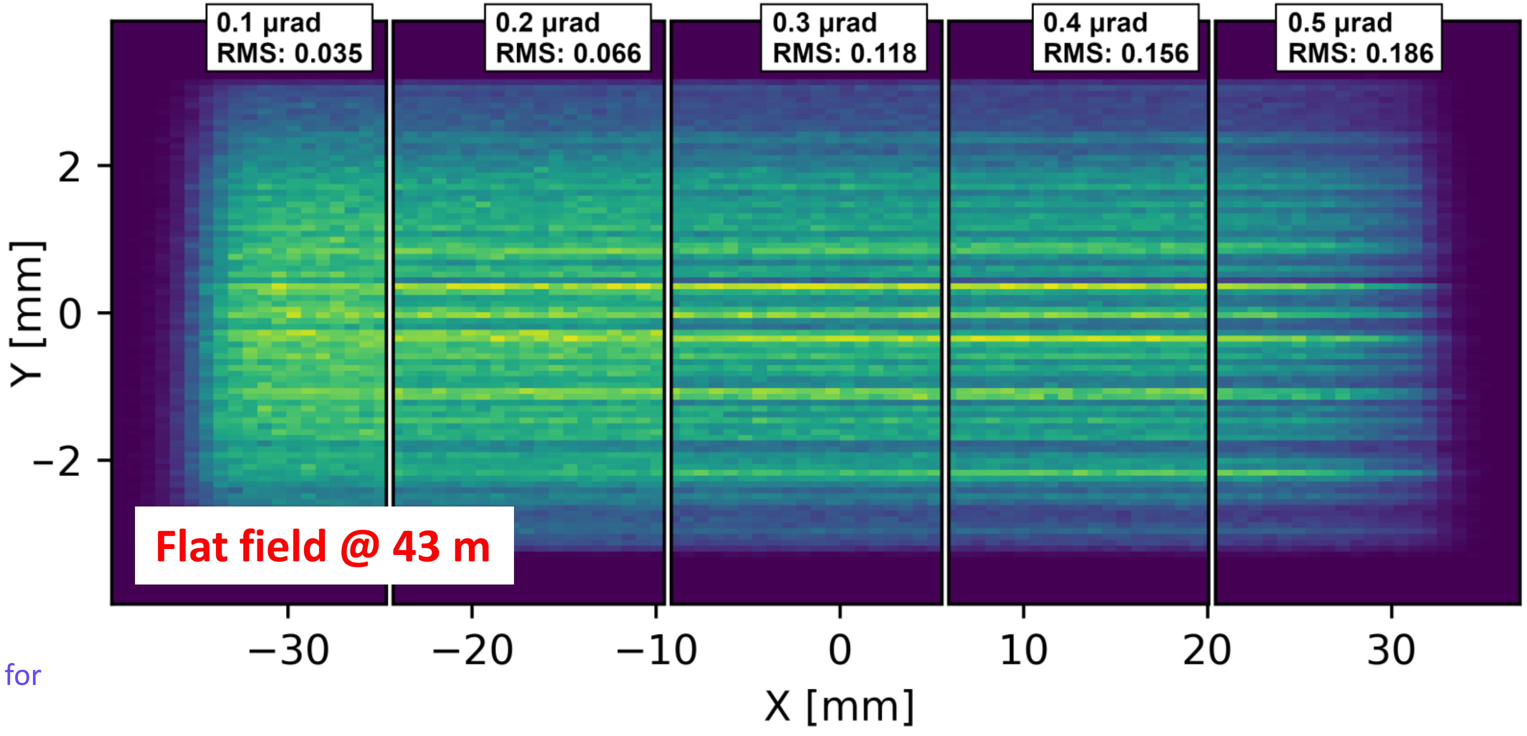

[A. Rack et al., "Comparative study of multilayers used in monochromators for synchrotron-based coherent hard X-ray imaging," J Synchrotron Rad. 2010]

BEATS – Installation status

- Infrastructure and hutches ready
- X-Ray source installation completed
- Exp. station installation: February 2022
- Start commissioning: March 2023

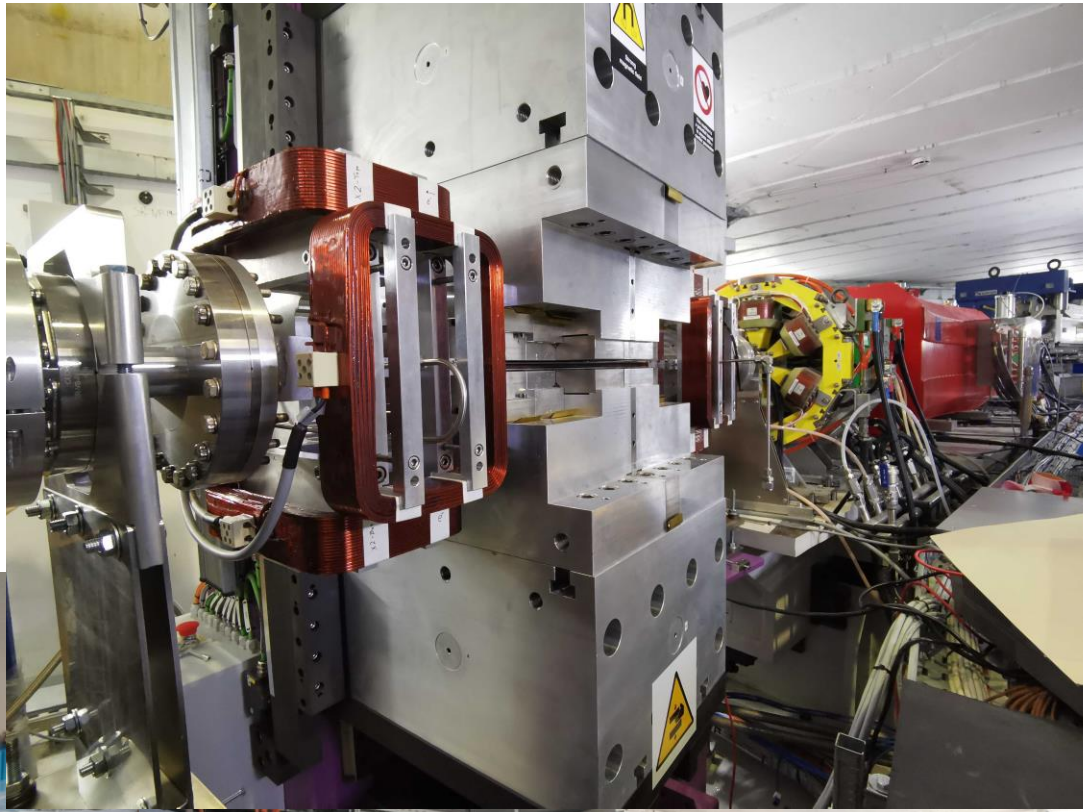

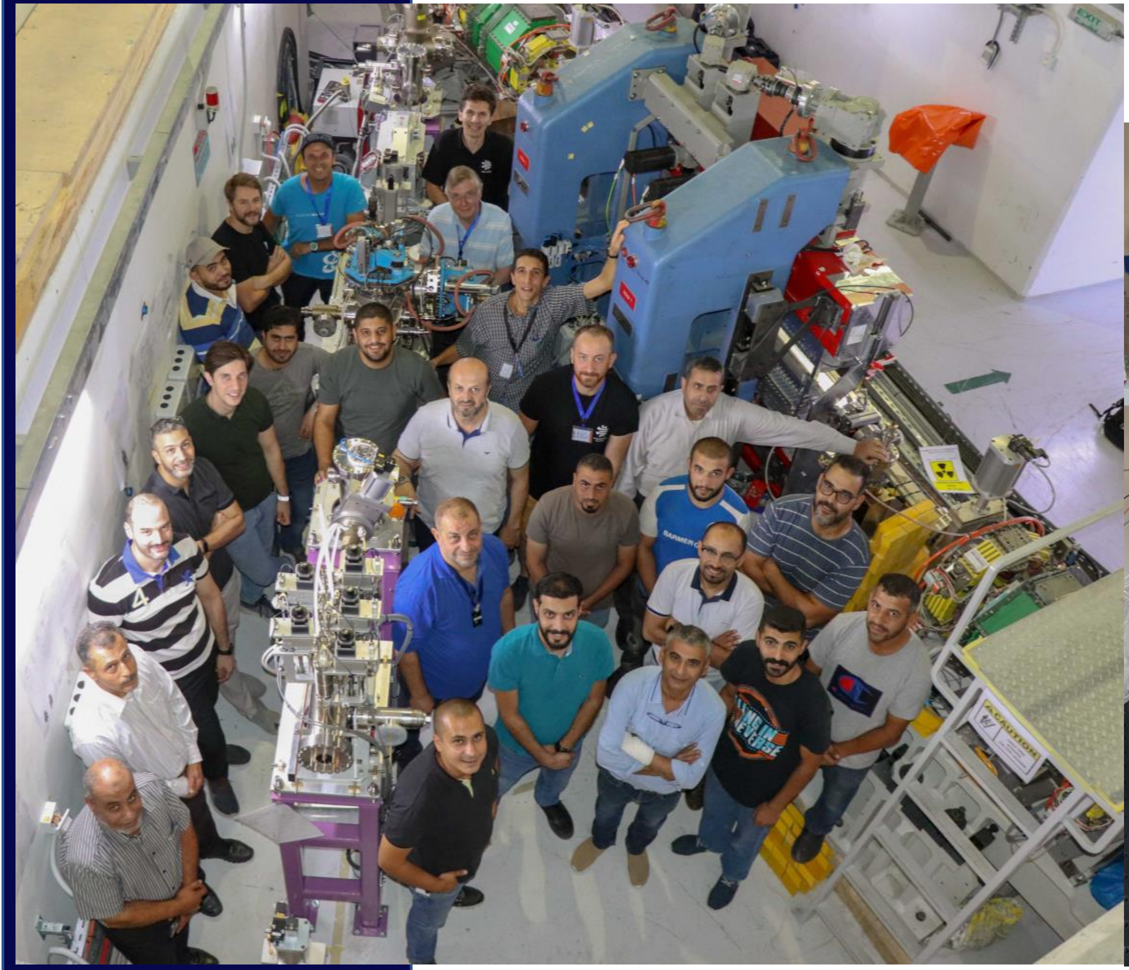

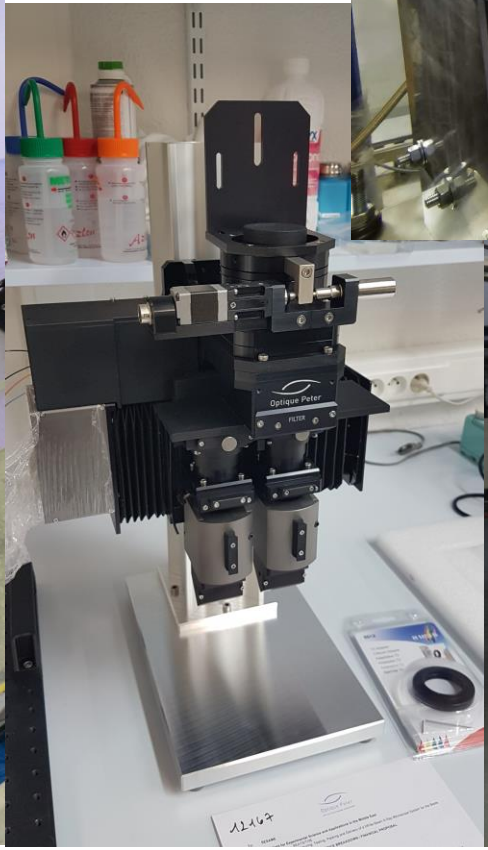

BEATS experimental station

Sample and detectors stage

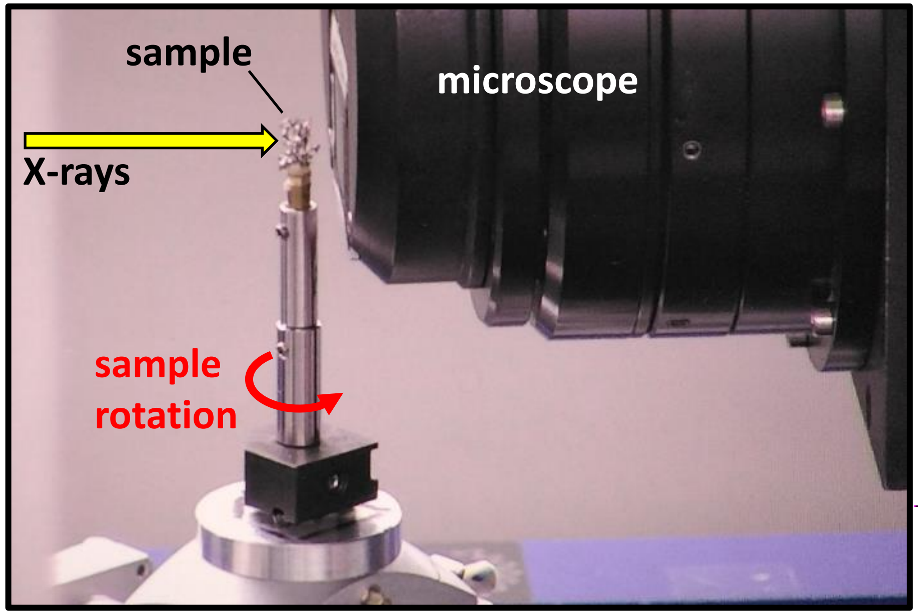

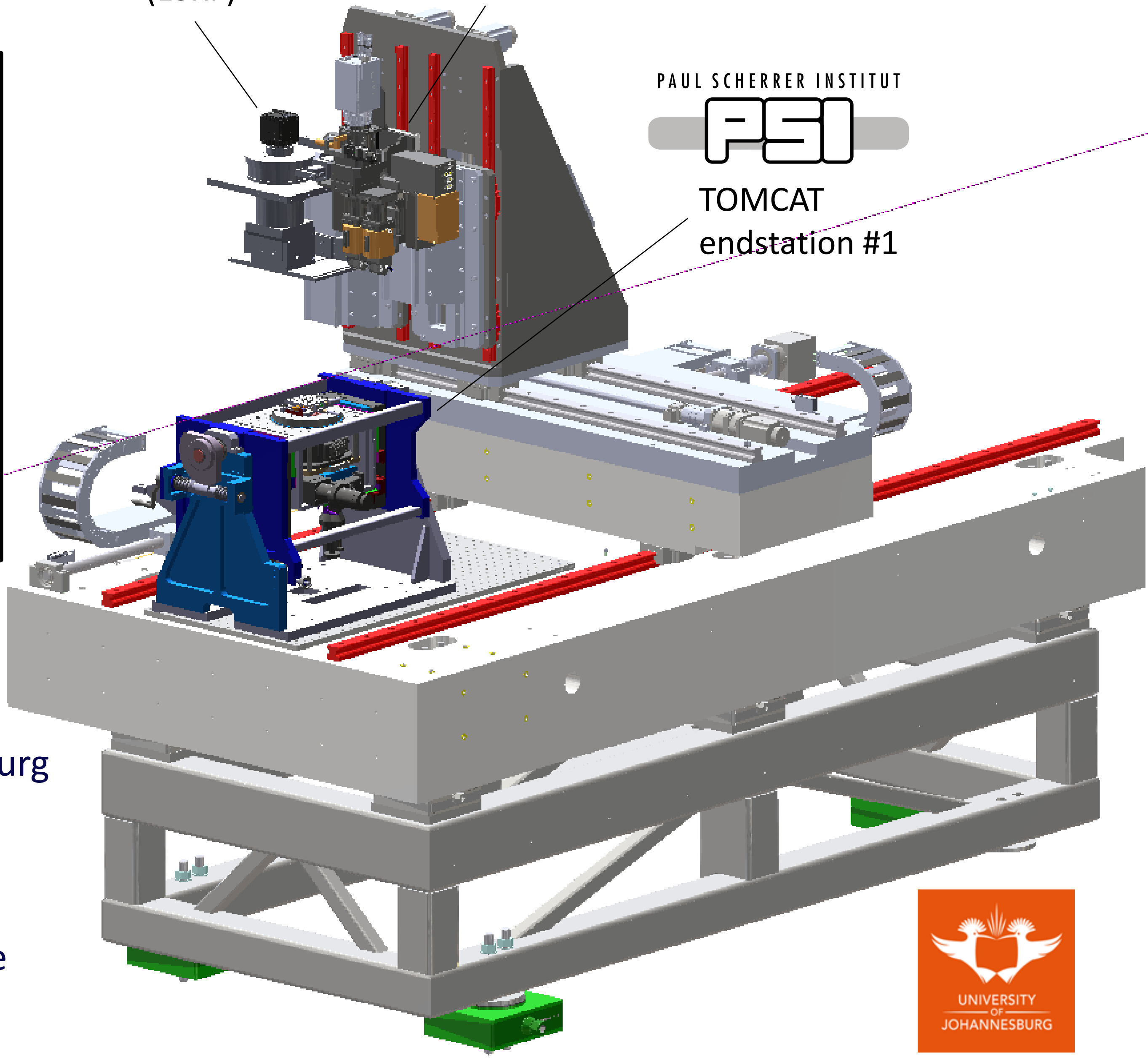

- Synergy with PSI TOMCAT, ESRF BM5 and UJ Johannesburg
- Air-bearing rotator for samples up to 5 kg
- Support for 2 detectors

- 1^{st} eigenmode of granite stage maximized to reduce the effect of vibrations on the detectors.

Magnif.	Field of view	Pixel size
0.5×	33.2 × 28.0 mm^2	13.0 µm
1×	16.6 × 14.0 mm^2	6.5 µm
2×	8.3 × 7.0 mm^2	3.25 µm
5×	3.4 × 2.8 mm^2	1.3 µm
10×	1.7 × 1.4 mm^2	0.65 µm

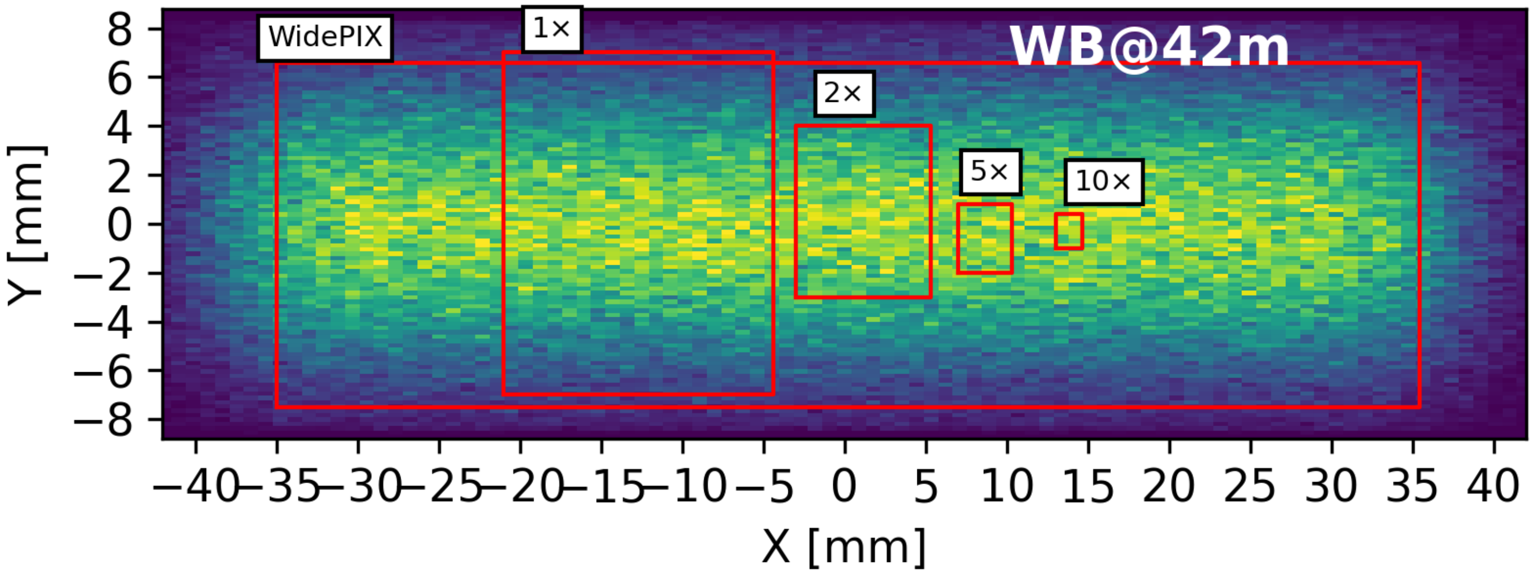

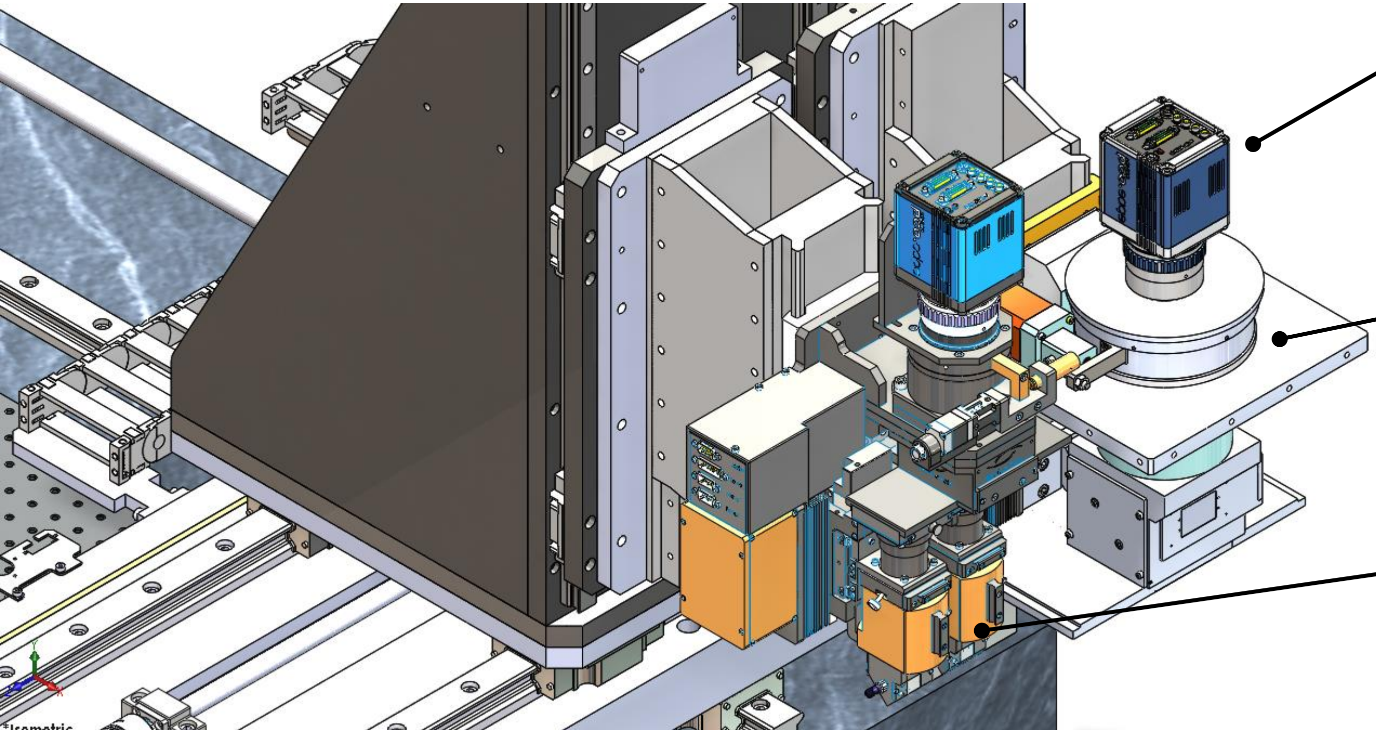

BEATS experimental station

X-Ray microscope

- Absorption efficiency of different scintillator screens of 350 μm thickness

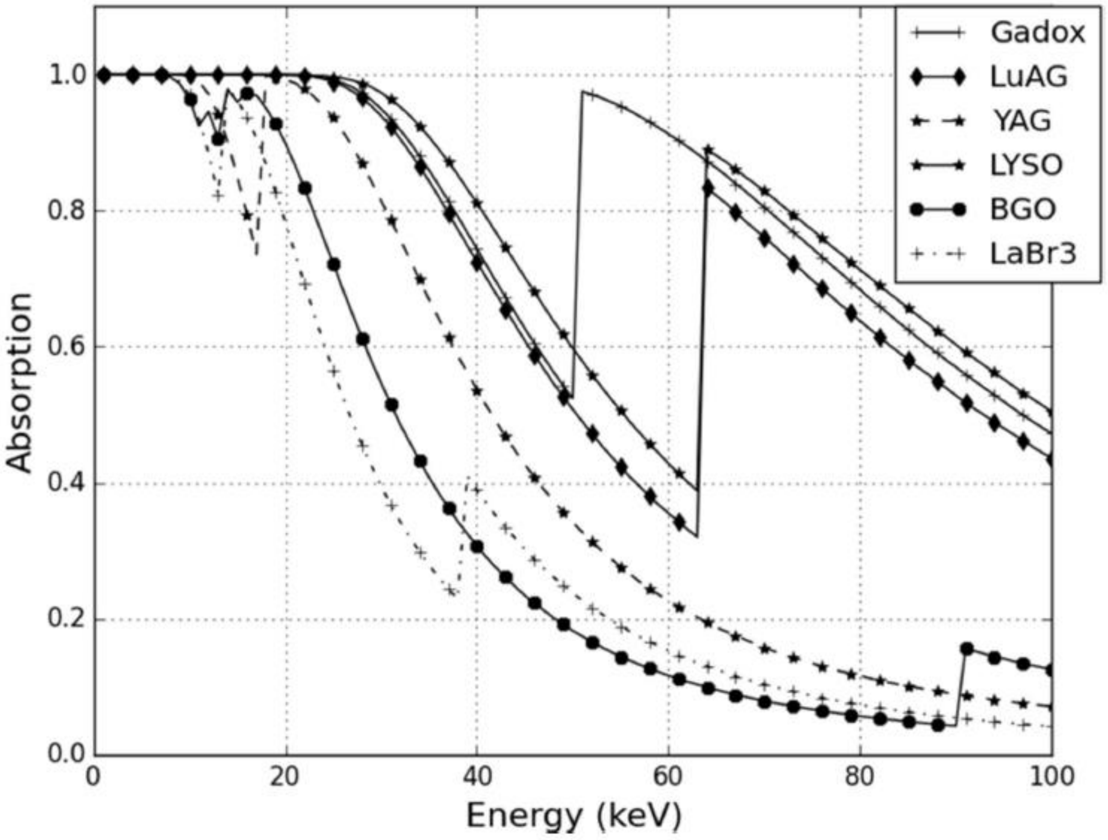

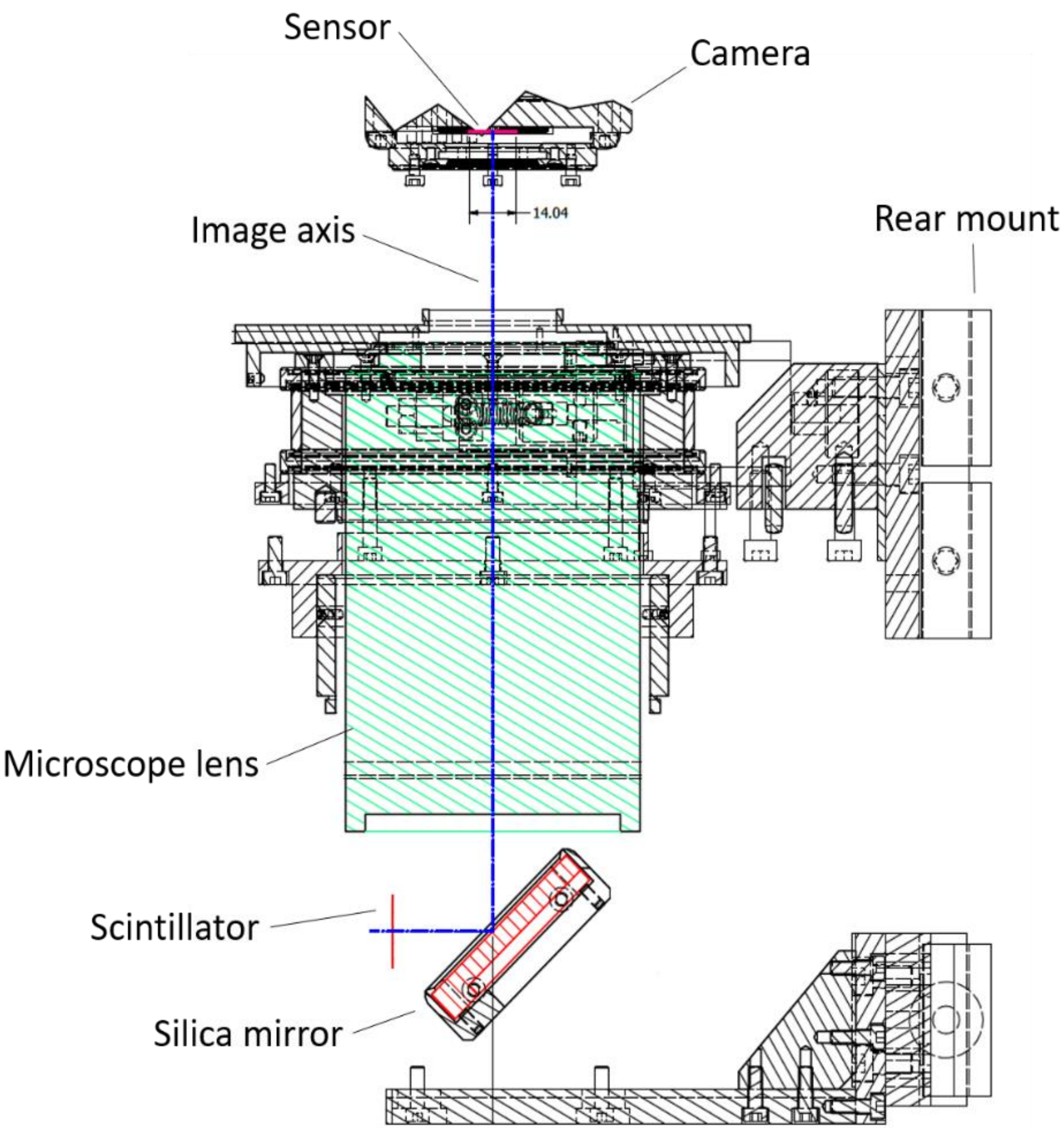

[A. Mittone et al. Journal of Synchrotron Radiation, 2017]

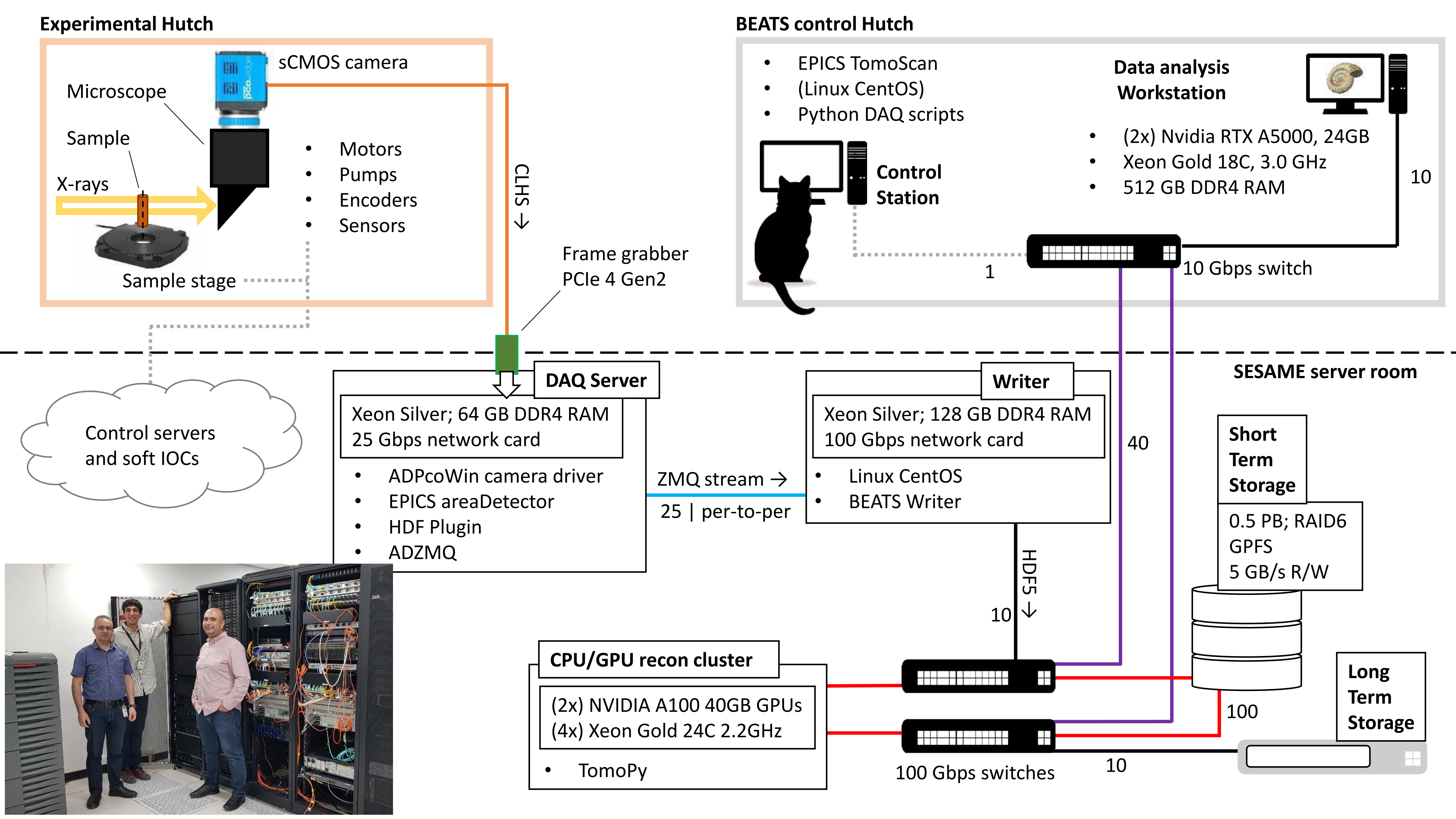

Experimental Hutch
sCMOS camera
Microscope
Sample
X-rays
Sample stage
Motors
Pumps
Encoders
Sensors
CLHS →
Frame grabber
PCIe 4 Gen2
BEATS control Hutch
EPICS TomoScan
(Linux CentOS)
Python DAQ scripts
Control Station
Data analysis Workstation
(2x) Nvidia RTX A5000, 24GB
Xeon Gold 18C, 3.0 GHz
512 GB DDR4 RAM
10
1
10 Gbps switch
SESAME server room
Control servers and soft IOCs
DAQ Server
Xeon Silver; 64 GB DDR4 RAM
25 Gbps network card
ADPcoWin camera driver
EPICS areaDetector
HDF Plugin
ADZMQ
ZMQ stream →
25 | per-to-per
Writer
Xeon Silver; 128 GB DDR4 RAM
100 Gbps network card
Linux CentOS
BEATS Writer
40
HDF5 →
10
Short Term Storage
0.5 PB; RAID6
GPFS
5 GB/s R/W
CPU/GPU recon cluster
(2x) NVIDIA A100 40GB GPUs
(4x) Xeon Gold 24C 2.2GHz
TomoPy
100
100 Gbps switches
10
Long Term Storage

Scientific Opportunities at BEATS

Archaeology and Cultural Heritage
- Archaeological Materials
- Human bioarchaeology
- Plant remains
- Animal remains and artefacts

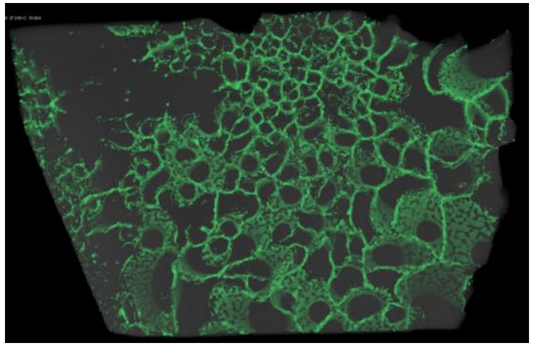
Roman glass

Mineralized algae
(red sea)

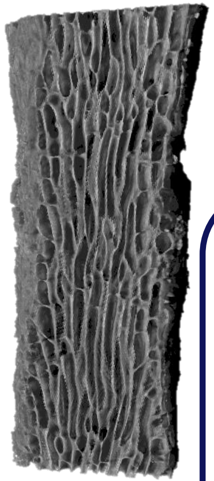


Bone implant

Health, Biology and Food
- Musculoskeletal research
- Bone and dental implants
- Soft tissue imaging
- Animal and plant characterization
- Food science

Synchrotron Tomography @ BEATS

Agriculture and Environment
- Simulation of rock properties
- Soil characterization
- Sustainable agriculture

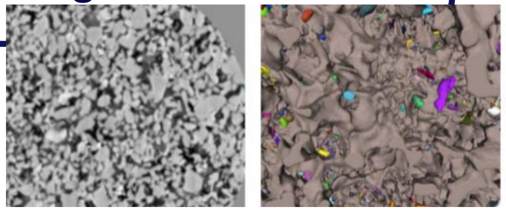
Sandstone core

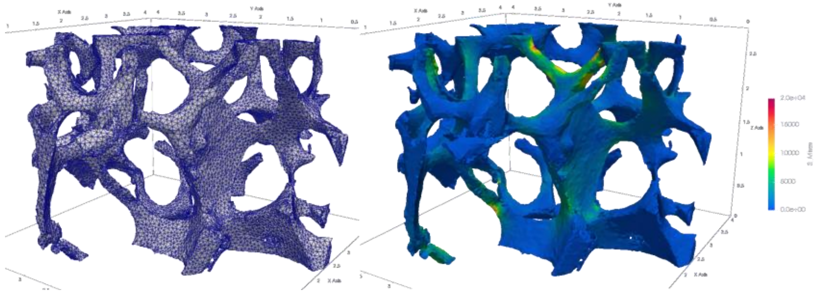

Material science and Engineering
- Light materials and alloys
- Materials under mechanical stress
- Energy materials research

Services to Industry and Private sector

Funded by the EU's H2020 framework programme under grant agreement n°822535

BEATS

BEAmline for Tomography at SESAME

Funded by the EU's H2020 framework programme under grant agreement n°822535

Scientific Opportunities at BEATS

Archaeology and Cultural Heritage:

- Archaeological Materials
  - Pottery and Ceramics
  - Glass
  - Textile
  - Wood
  - Manuscripts
- Plant remains
- Animal remains
  - Bone
  - Antler
  - Teeth
- Statues
- Ornaments

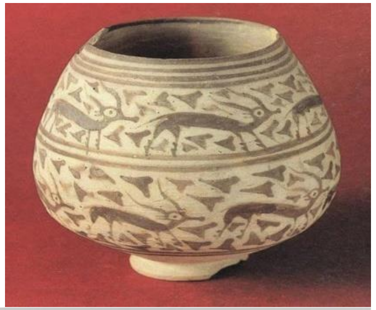

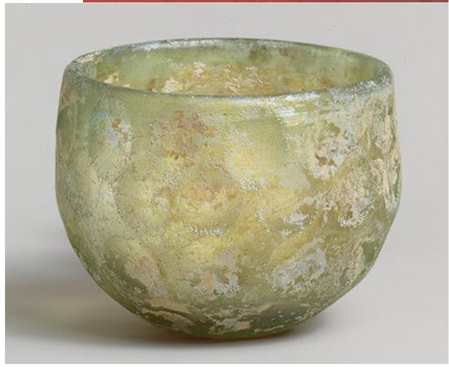

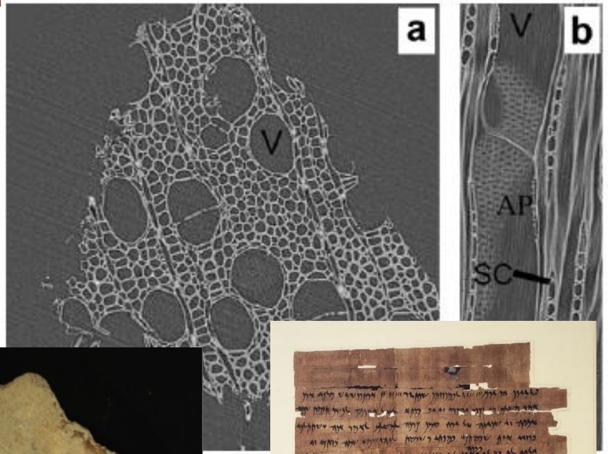

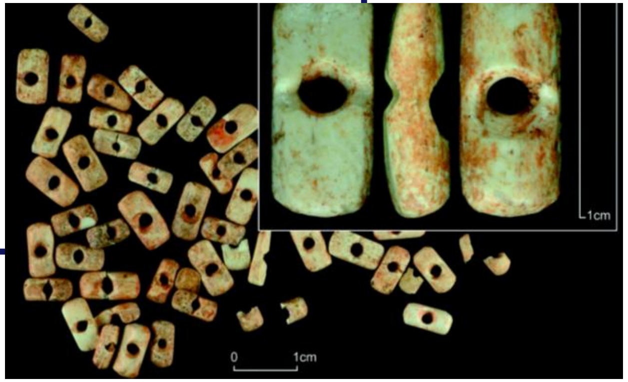

BEAmline for Tomography at SESAME

Scientific Opportunities at BEATS - Archaeology and Cultural Heritage

Rectangular Beads from the Abri Pataud: Raw Material Identification and Archaeological Implications

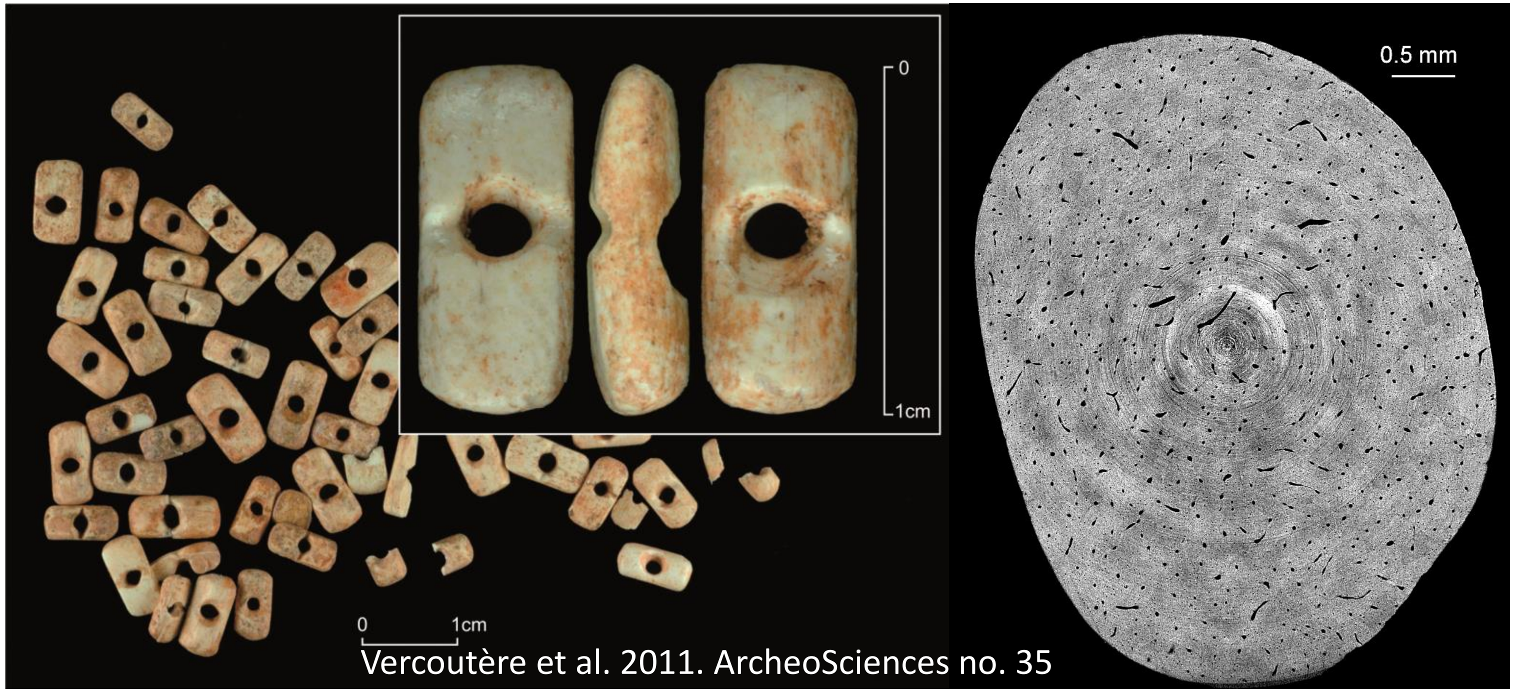

Vercoutère et al. 2011. ArcheoSciences no. 35

- BAMline@BESSY-II; absorbtion CT; 0.44 to 3.5 µm pixel size; 15 keV
- Mammoth ivory; upper paleolithic; abri Pataud, France
- Non-destructive material identification
- Applicable to ivory, bone, antler, faience, wood, and more..

Funded by the EU's H2020 framework programme under grant agreement n°822535

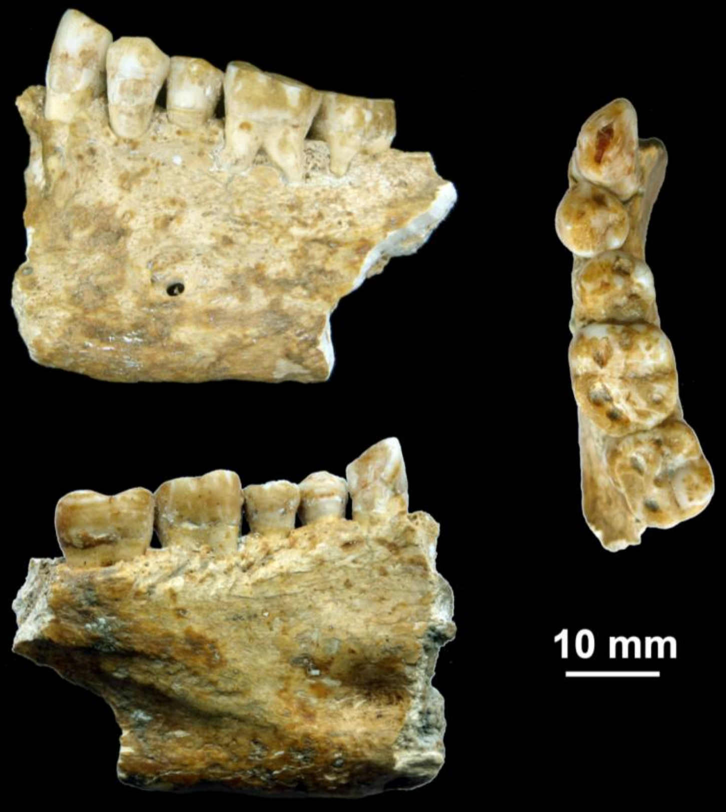

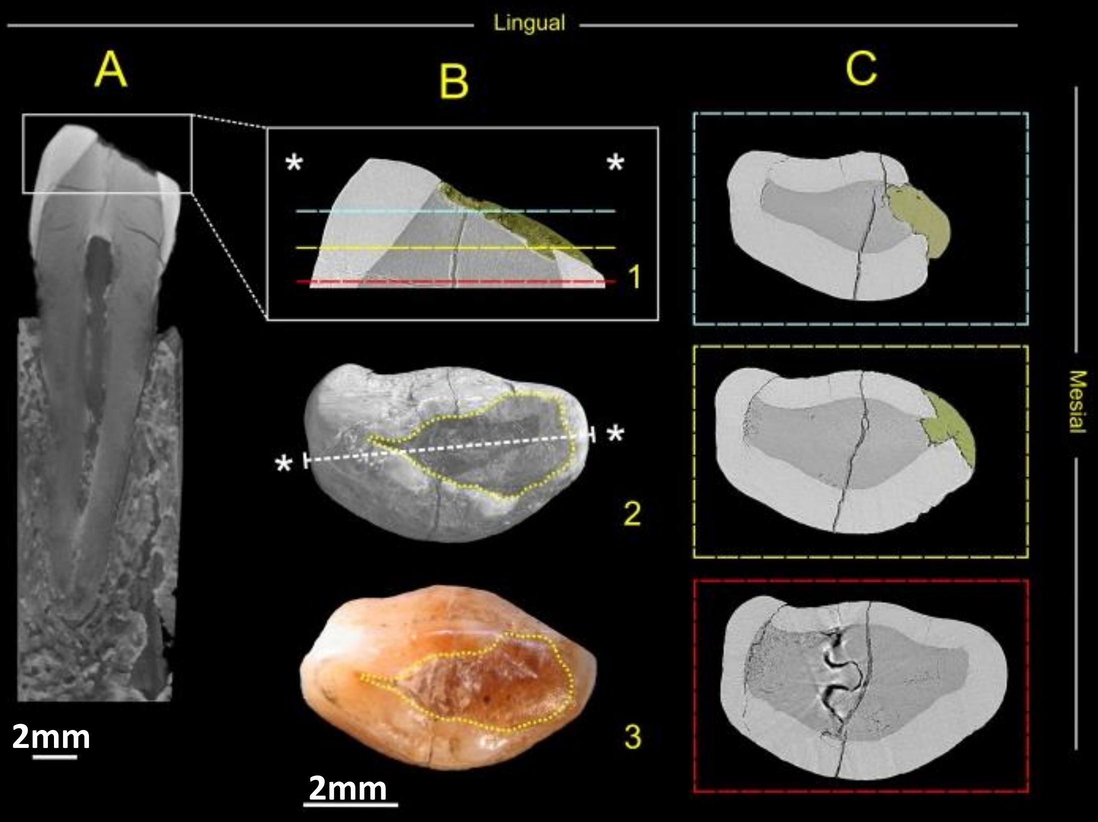

Beeswax as Dental Filling on a Neolithic Human Tooth. Bernardini et al. 2012. PLoS ONE 7 (9).
https://doi.org/10.1371/journal.pone.0044904

- The Lonche canine: lab XCT (resolution 18 µm) and phase-contrast SXCT (resolution 9 µm)
- Non-destructive 3D characterization of wear pattern and therapeutic-palliative dental filling

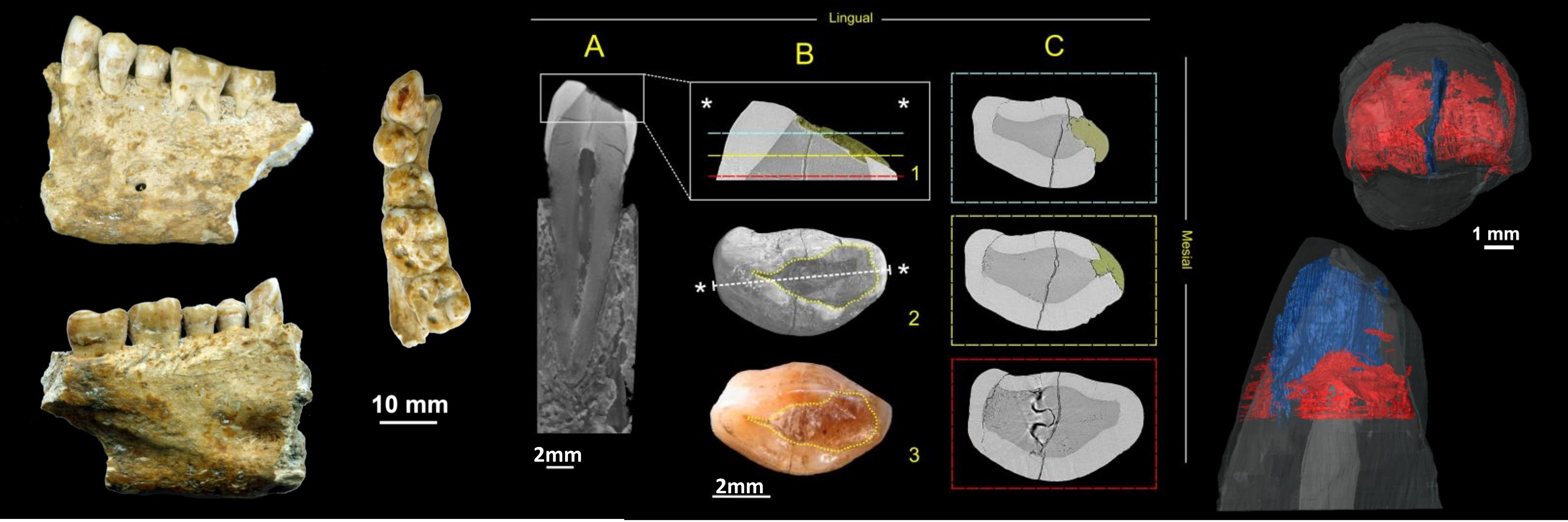

Beeswax as Dental Filling on a Neolithic Human Tooth. Bernardini et al. 2012. PLoS ONE 7 (9).
https://doi.org/10.1371/journal.pone.0044904

- The Lonche canine: lab XCT (resolution 18 µm) and phase-contrast SXCT (resolution 9 µm)
- Non-destructive 3D characterization of wear pattern and therapeutic-palliative dental filling

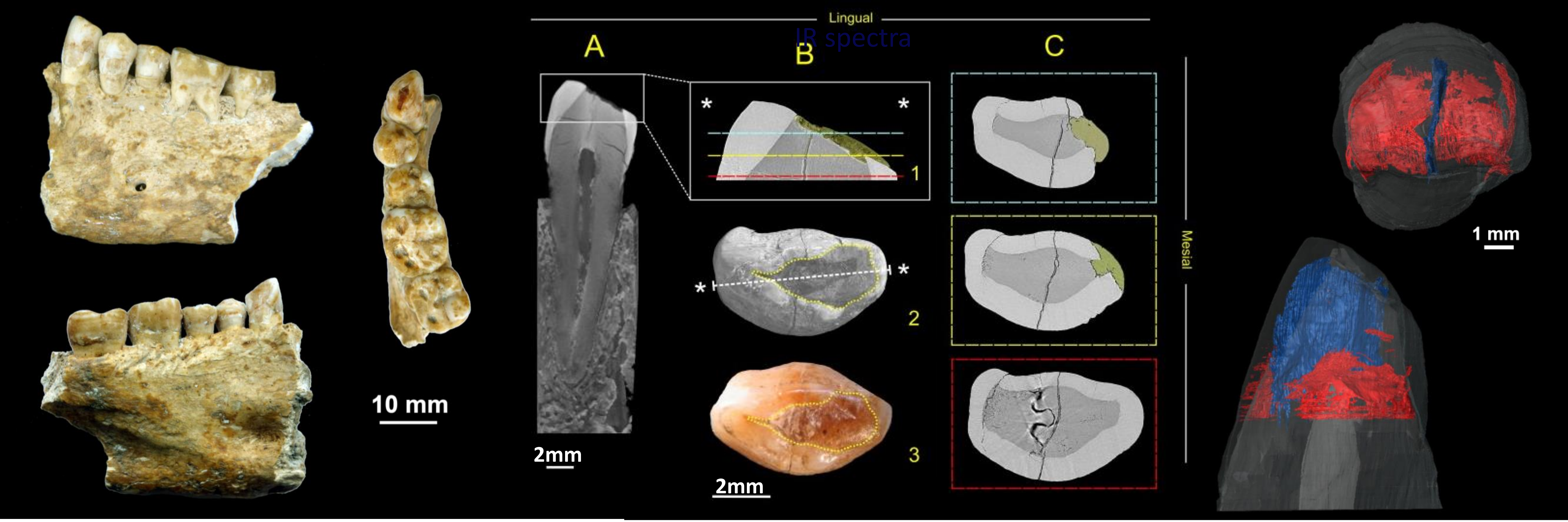

Beeswax as Dental Filling on a Neolithic Human Tooth. Bernardini et al. 2012. PLoS ONE 7 (9).
https://doi.org/10.1371/journal.pone.0044904

- The Lonche canine: lab XCT (resolution 18 µm) and phase-contrast SXCT (resolution 9 µm)
- Non-destructive 3D characterization of wear pattern and therapeutic-palliative dental filling
- FT-IR revealed composition of the filling (beeswax)
- Radiocarbon dating of mandible and dental filling demonstrated that the dental filling covers the canine occlusal surface since Neolithic times.

Scientific Opportunities at BEATS

BEAmline for Tomography at SESAME

Health, Biology and Food:

- Musculoskeletal research
- Bone and dental implants
- Soft tissue imaging
- Animal and plant characterization
- Food science

Coleoptera fossil

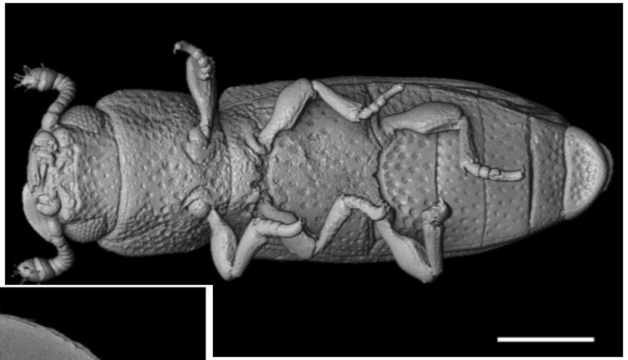

Green bean

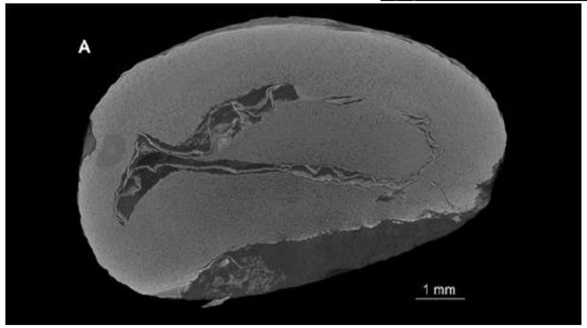

Mineralized algae (red sea)

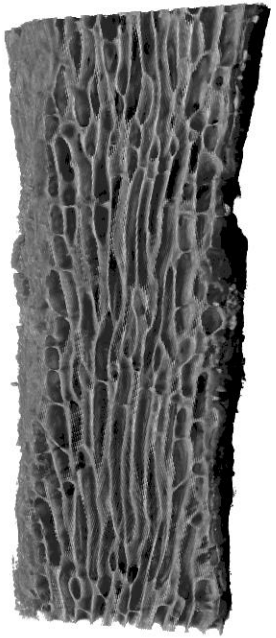

Bone implant

Dental implant

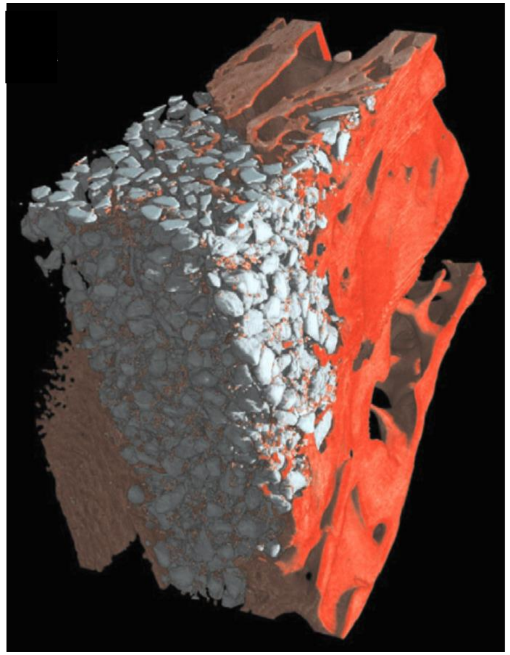

Caries

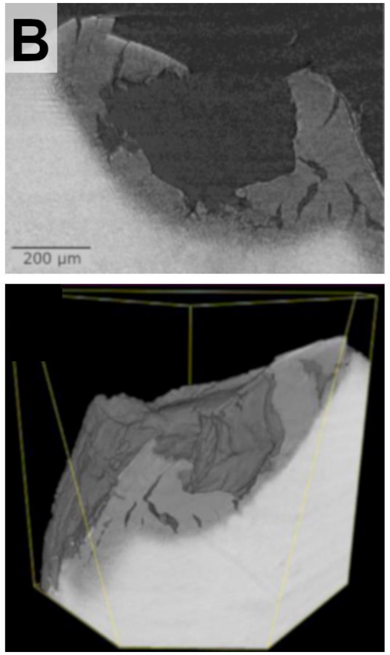

Scientific Opportunities at BEATS

Material science and Engineering:

- Energy materials research
- Concrete, fiber-composites, 3D printed materials
- Light materials and alloys
- Materials under mechanical stress
- From CT images to FE simulations

Light engineering materials (steel foam)

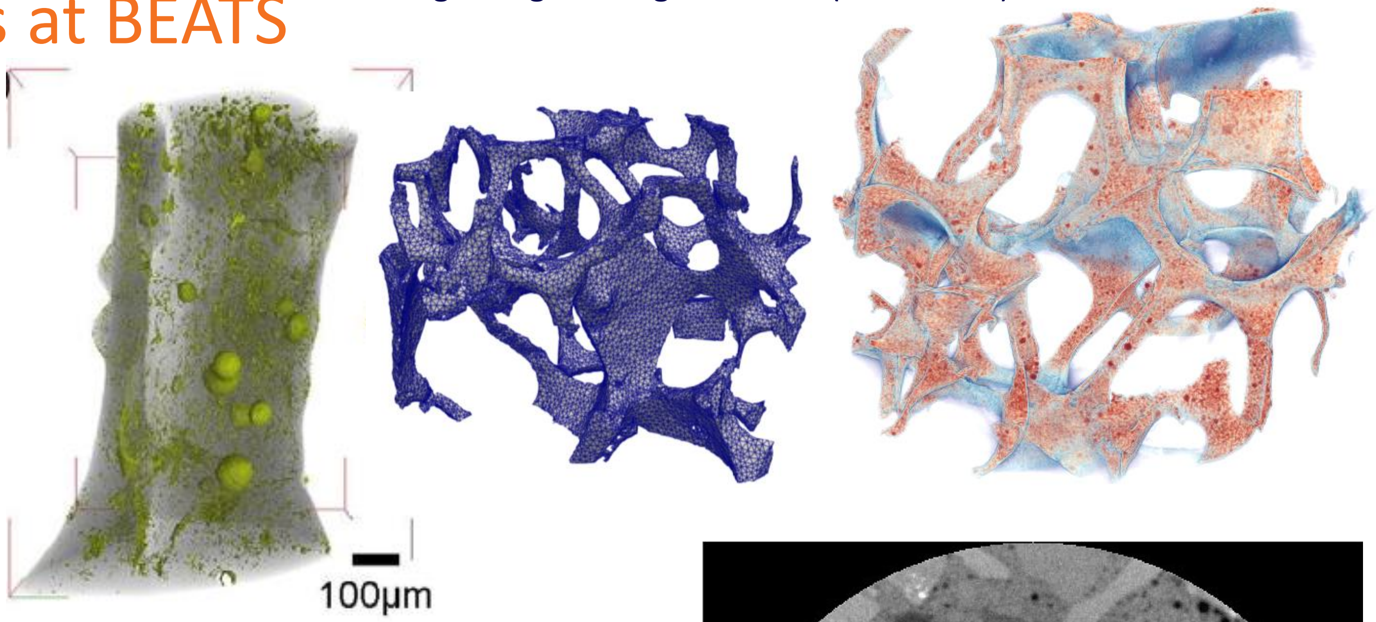

Advanced Engineering Materials 21, 1900080 (2019).
Kaya, A. et. Al. Foams of Gray Cast Iron as Efficient Energy Absorption Structures: A Feasibility Study.

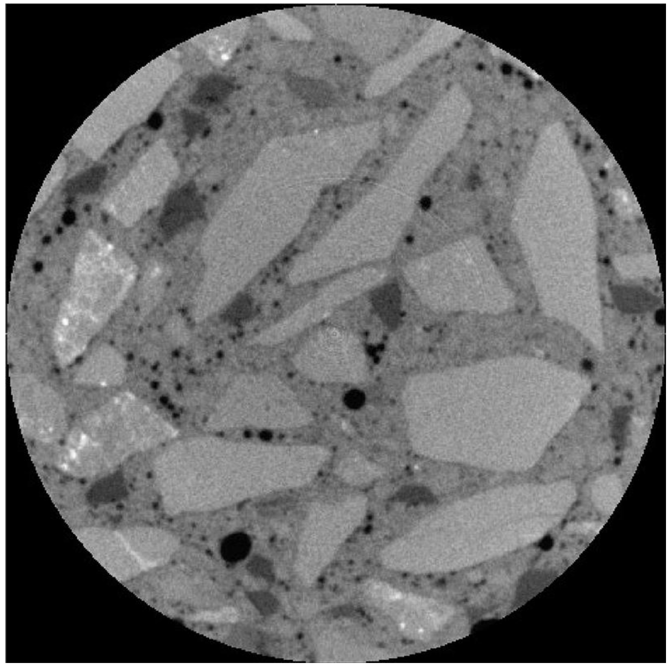

Liu Z. et al. J. of Cleaner Production (2021).

Micro-structure of self-compacting concrete modified by recycled grinded tire rubber based

Prates Soares et al. J. of Synchrotron Rad. (2020).

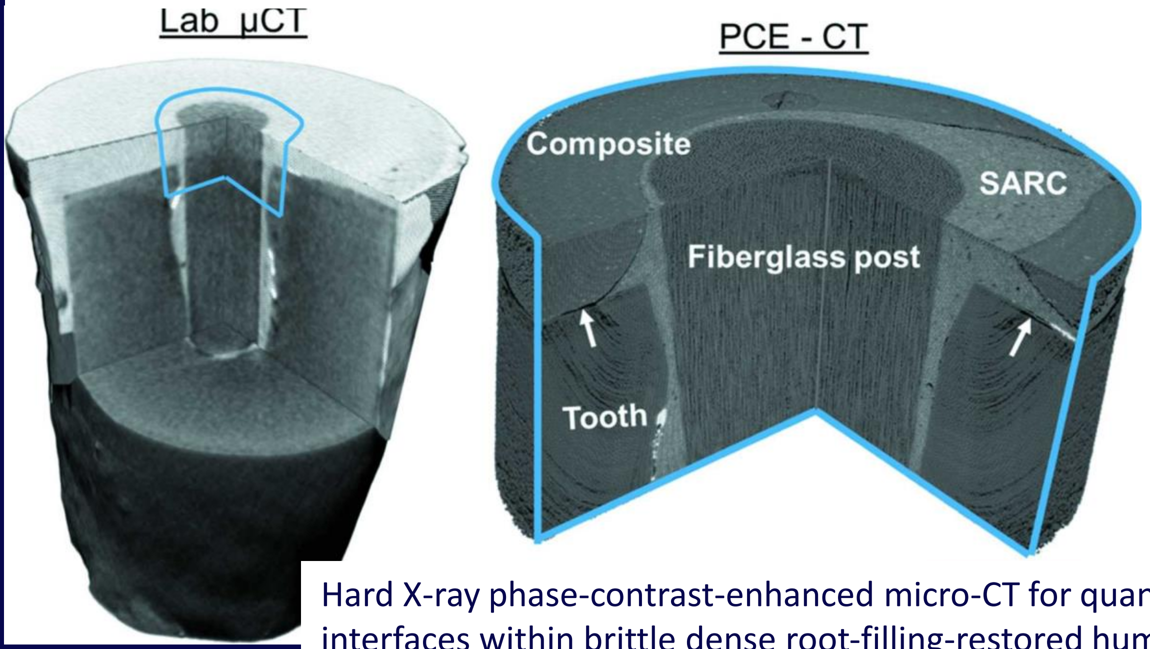

Hard X-ray phase-contrast-enhanced micro-CT for quantifying interfaces within brittle dense root-filling-restored human teeth.

Tomography 3D rendering of a non-uniform hollow strut and overlay of the observed embedded micro/macropores in green

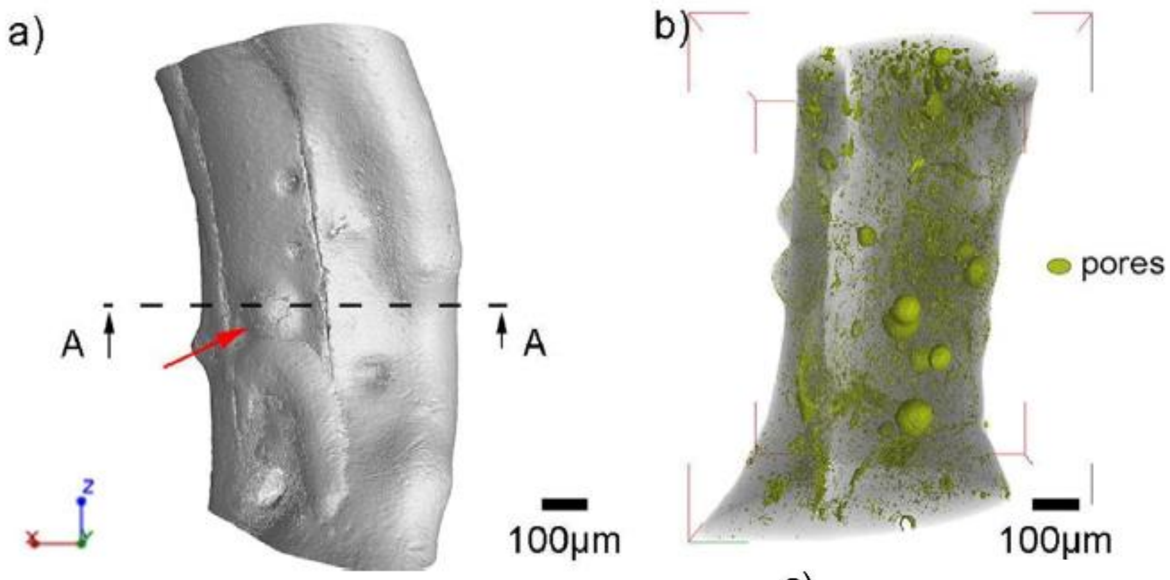

BEFORE loading

AFTER loading

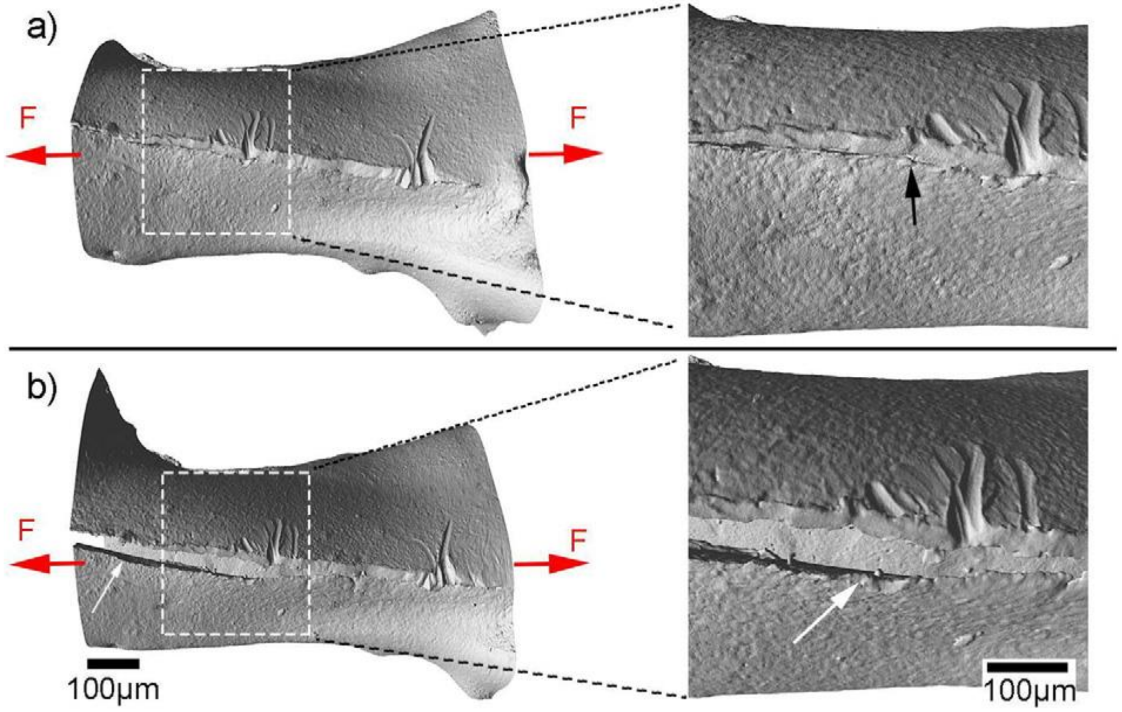

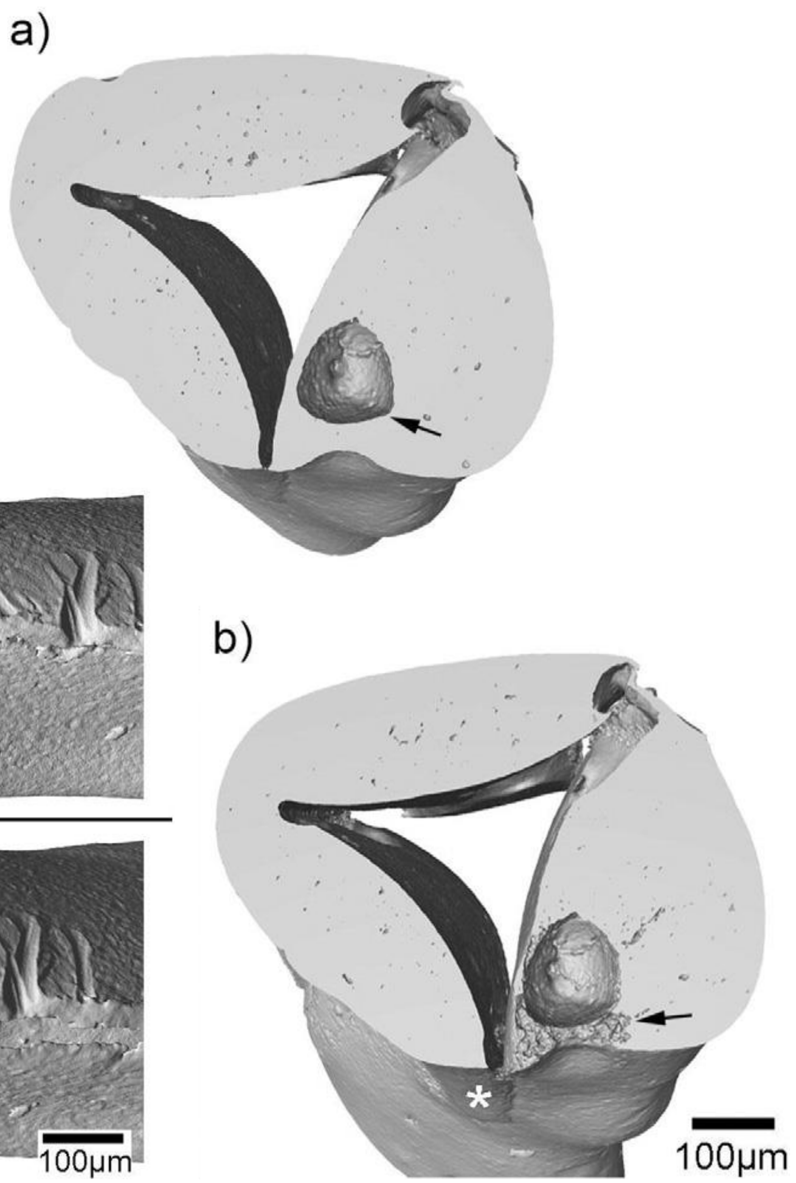

Advanced Engineering Materials 21, 1900080 (2019).
Kaya, A. et. Al. Foams of Gray Cast Iron as Efficient Energy Absorption Structures: A Feasibility Study.

From synchrotron tomography data to FE models

Tomography scan

↓

Segmentation

↓

Meshing

↓

Material mapping and Boundary Conditions

↓

FE solution

↓

FE post-processing

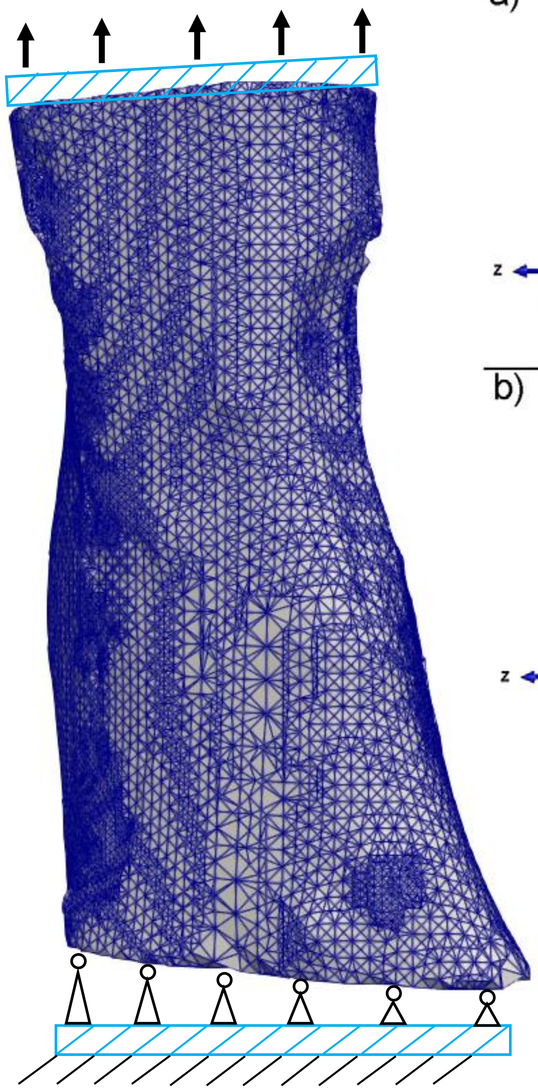

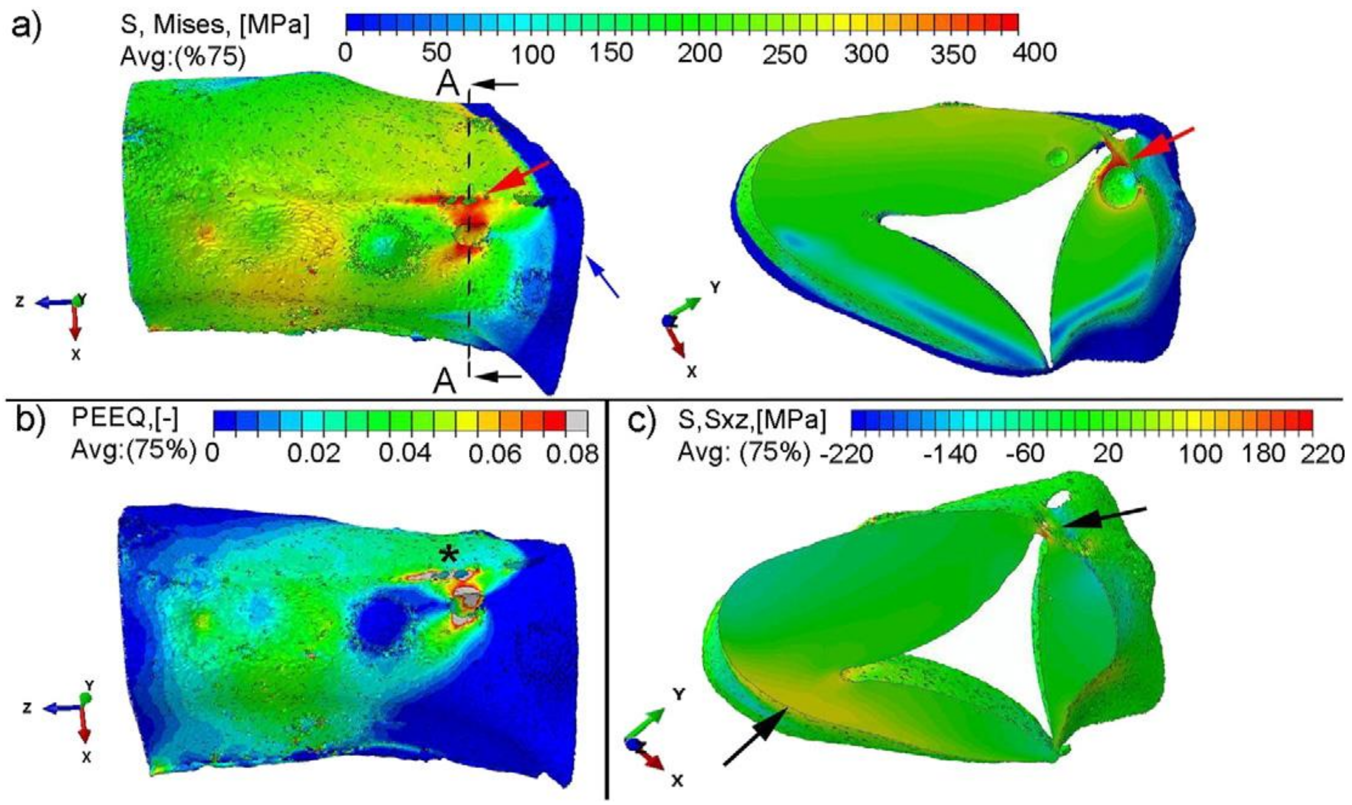

Advanced Engineering Materials 21, 1900080 (2019).
Kaya, A. et. Al. Foams of Gray Cast Iron as Efficient Energy Absorption Structures: A Feasibility Study.

Sample environments for in-situ studies

Sample furnace – Induction heating

- Enables control of sample environment during heating
- Superior control of heating gradient up to 1800 C
- Requires slip ring for coolant and flushing with inert gas

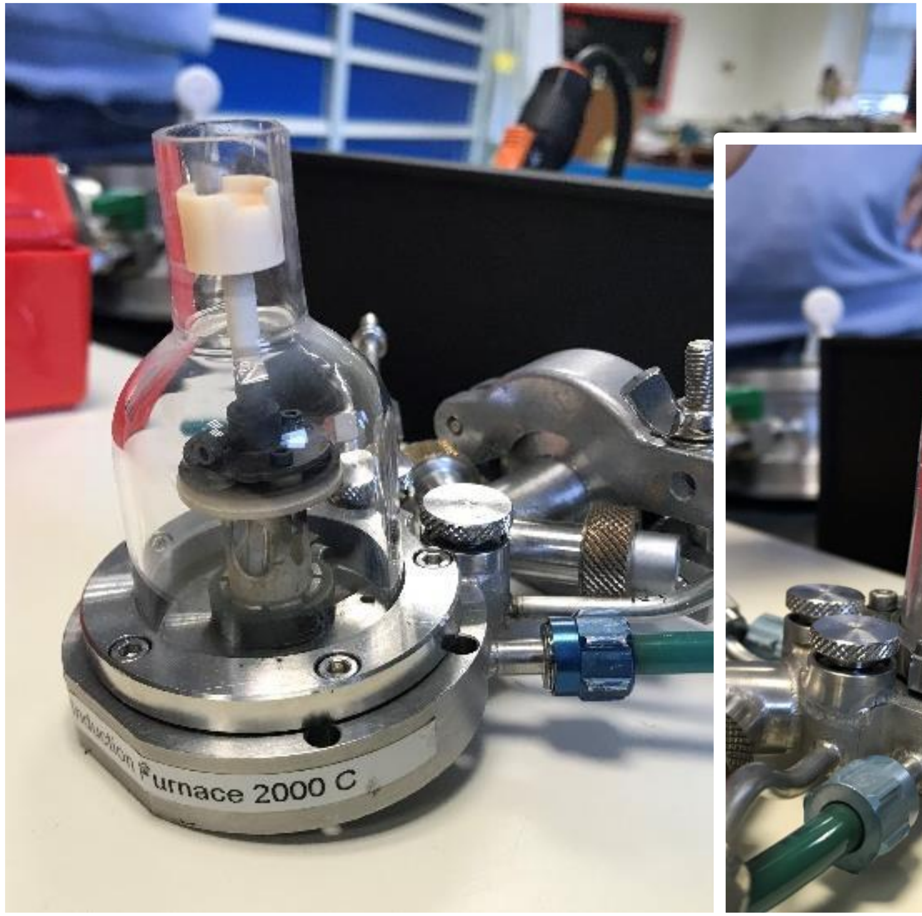

[F. Mokoena, M.Sc. thesis]

Sample environments for in-situ studies

Sample furnace – Induction heating

- Design optimization:
  - Crucible architecture
  - Temperature control and convection regime around sample
  - Isolation of slip ring and sensitive equipment
  - Simulate different sample materials and sizes
  - Predict cooling flow rate for experiments at the beamline

Fortune Mokoena

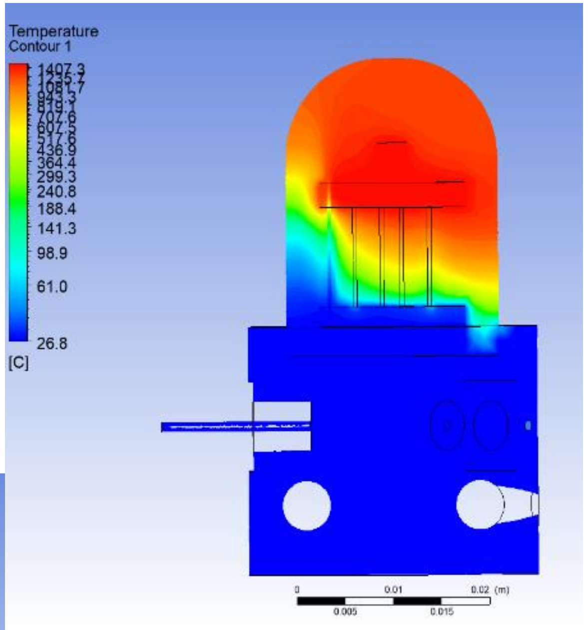

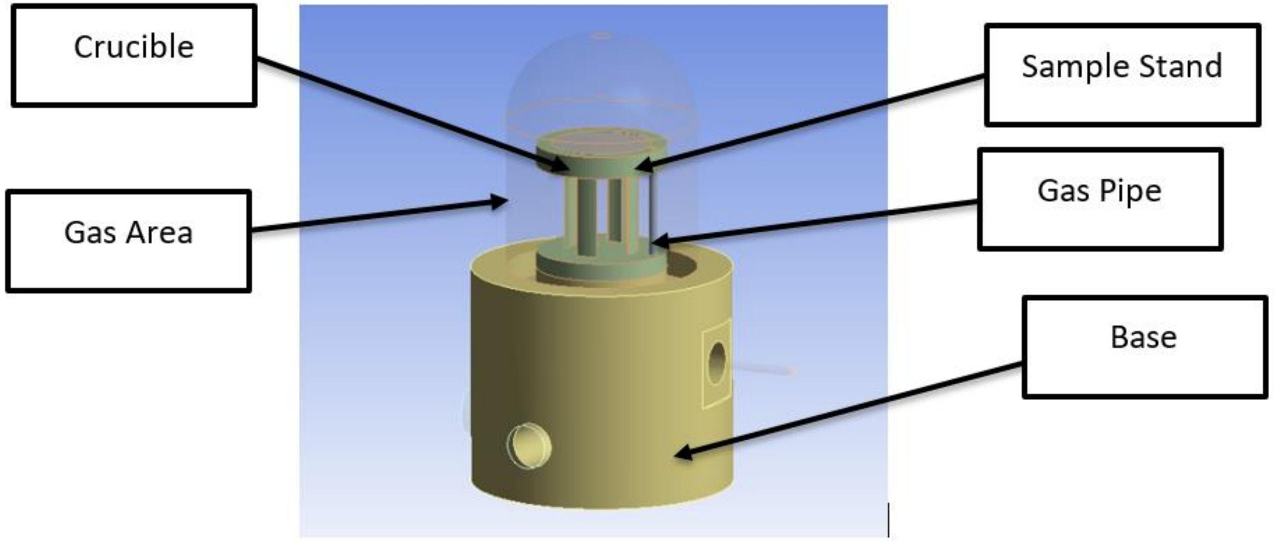

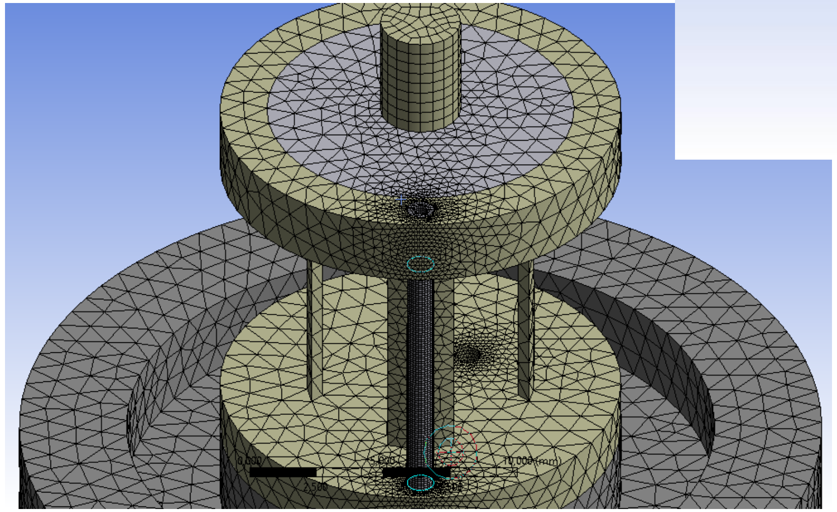

[F. Mokoena, M.Sc. thesis]

BEATS

BEAmline for Tomography at SESAME

Scientific Opportunities at BEATS

Agriculture and Environment
- Quantification of rock properties
- Soil characterization
- Sustainable agriculture

Permeability of sandstone core

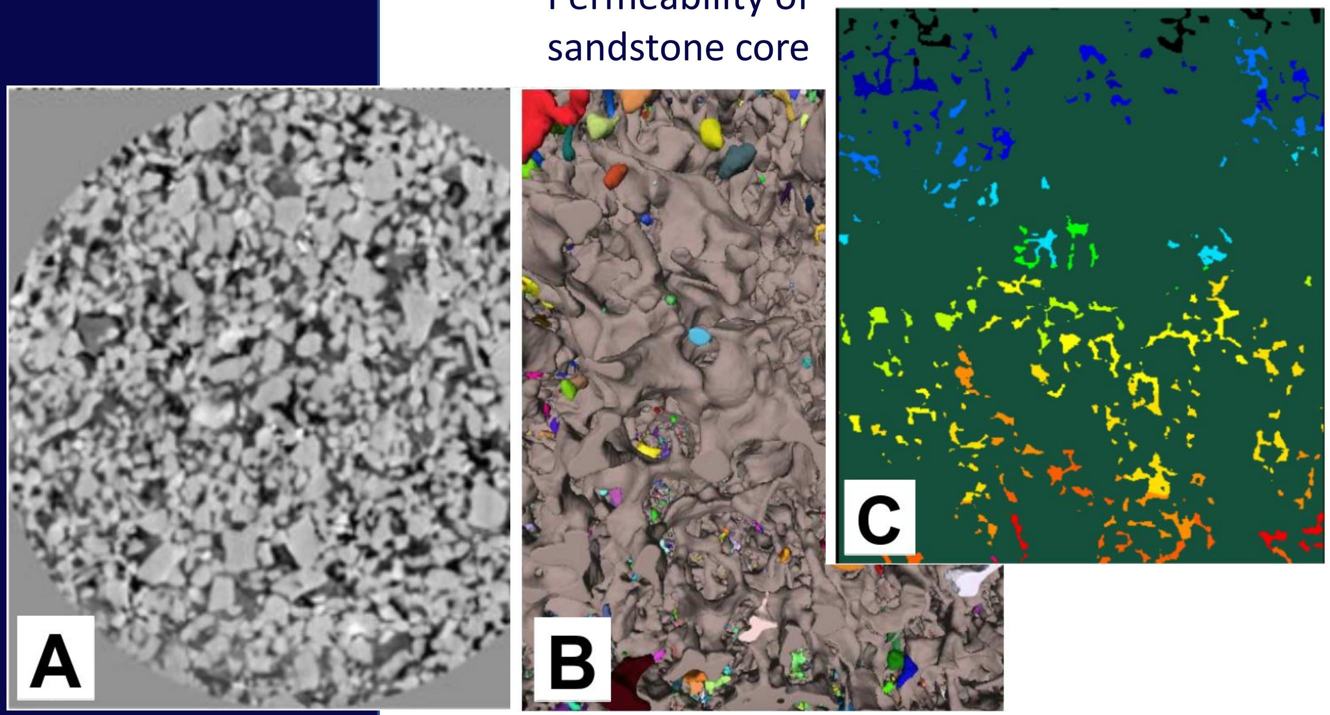

Kakouie, A. et al. Unpublished. Courtesy Shiva Shirani.

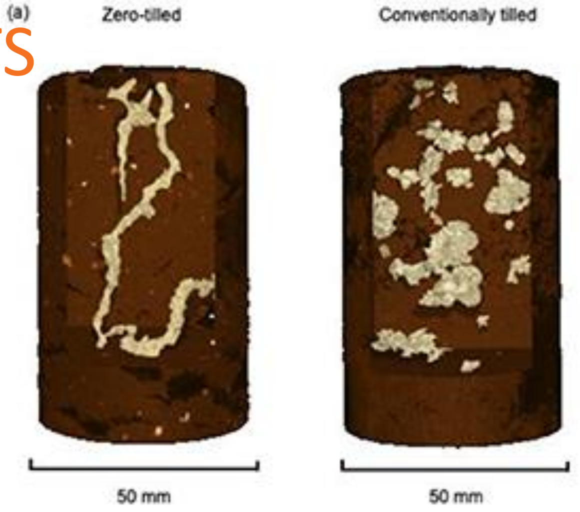

Cooper, H V. et al. Environ. Res. Letters (2021).

Excessive soil tillage associated with soil degradation processes: compaction, decrease in soil stability, increased soil erosion.

Inorganics, pores + organics

Pores + organics

Pores

Organics

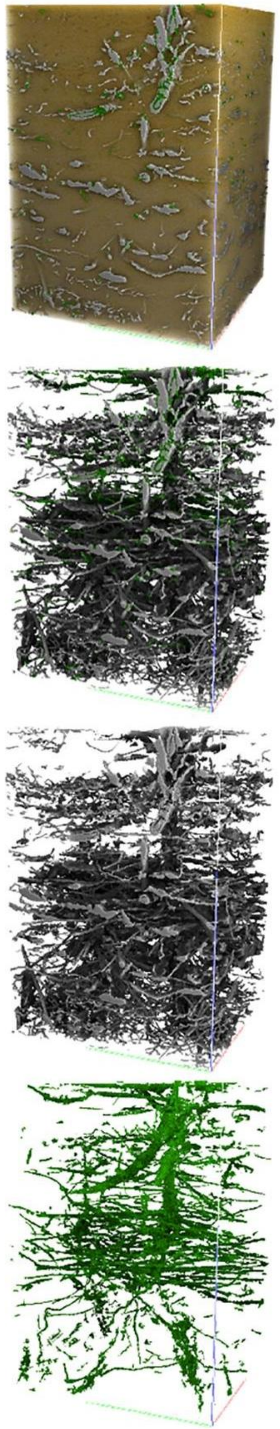

Chirol, C. et al. Geoderma (2021).

Pore, live root and inorganic quantification in complex heterogeneous wetland soils using XCT

Unlocking History through Automated Virtual Unfolding of Sealed Documents Imaged by XCT.
Dambrogio et al. 2021. Nature Communications 12 (1): 1–10.
https://doi.org/10.1038/s41467-021-21326-w

- Before the proliferation of envelopes in the 1830s, most letters were sent via **letterlocking**, the process of folding and securing writing substrates to become their own envelopes.
- **Reverse-engineering historical letterpackets and letterlocking** can provide key datasets for the study of historical communications security methods.

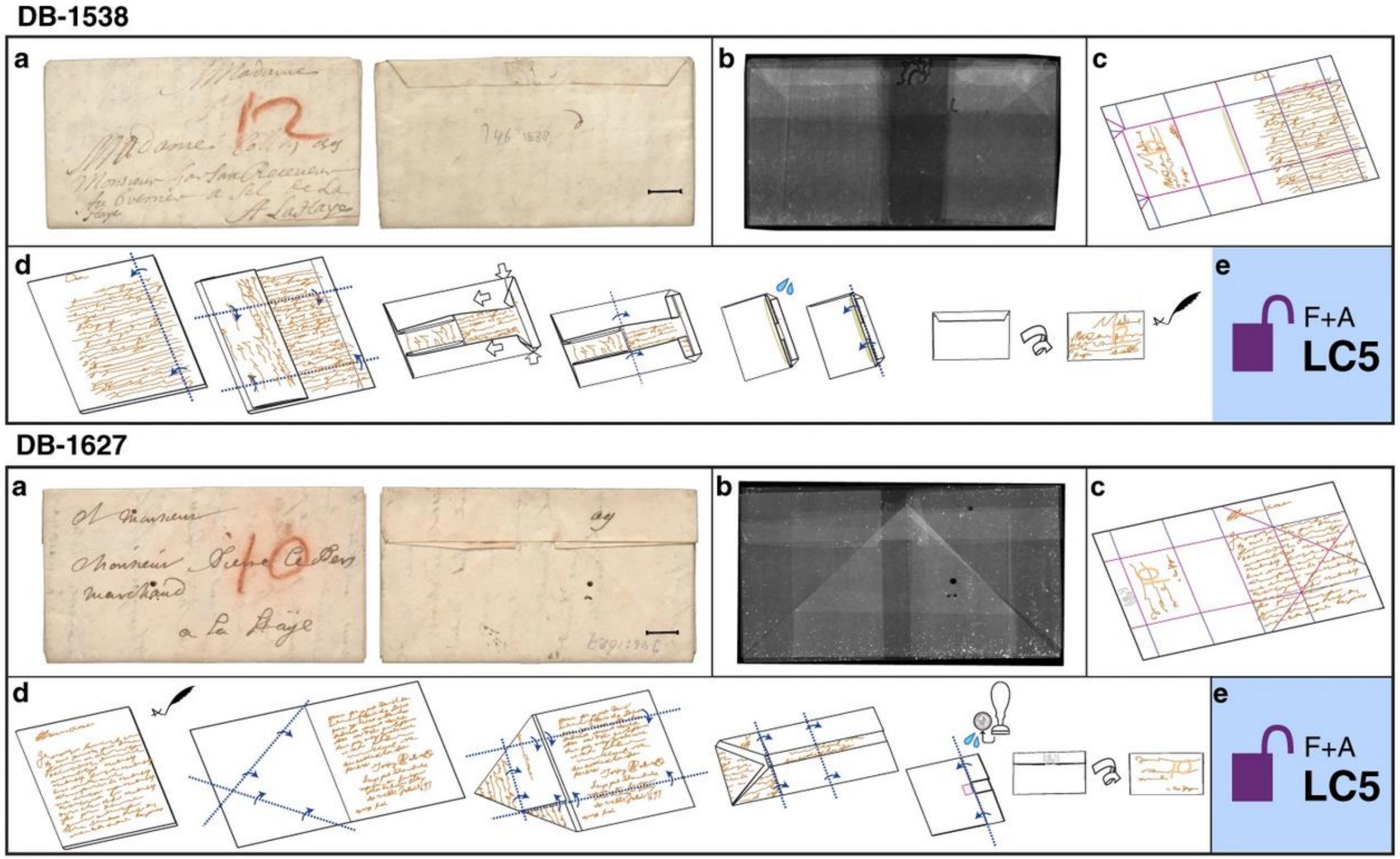

Unlocking History through Automated Virtual Unfolding of Sealed Documents Imaged by XCT.
Dambrogio et al. 2021. Nature Communications 12 (1): 1–10.
https://doi.org/10.1038/s41467-021-21326-w

- Fully automatic computational approach for reconstructing and virtually unfolding volumetric scans of a locked letter with complex internal folding

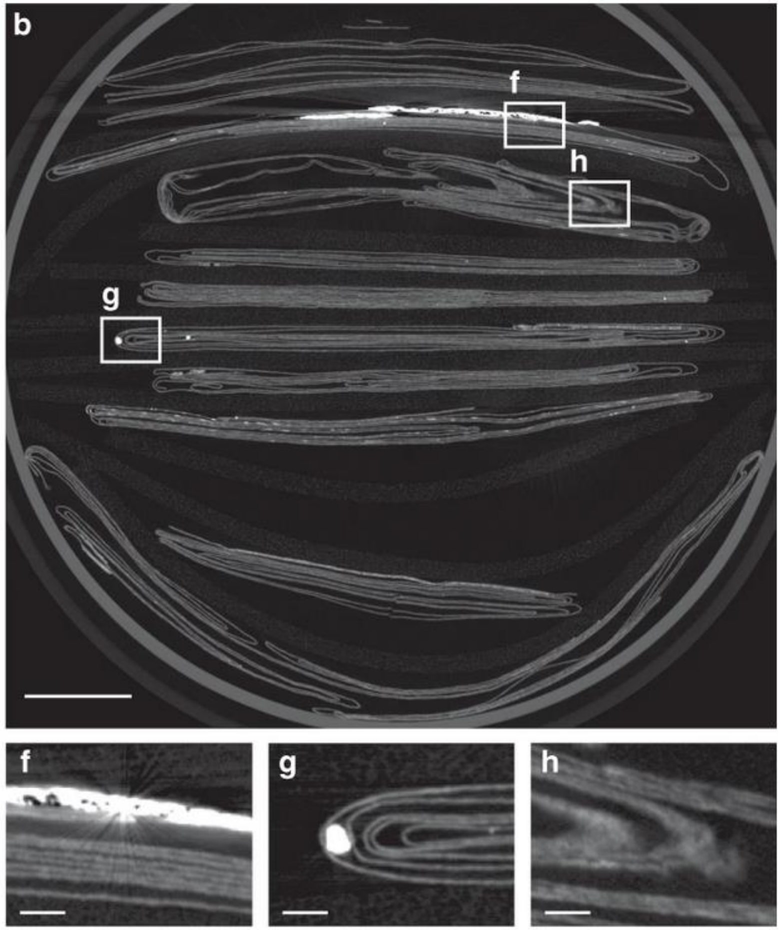

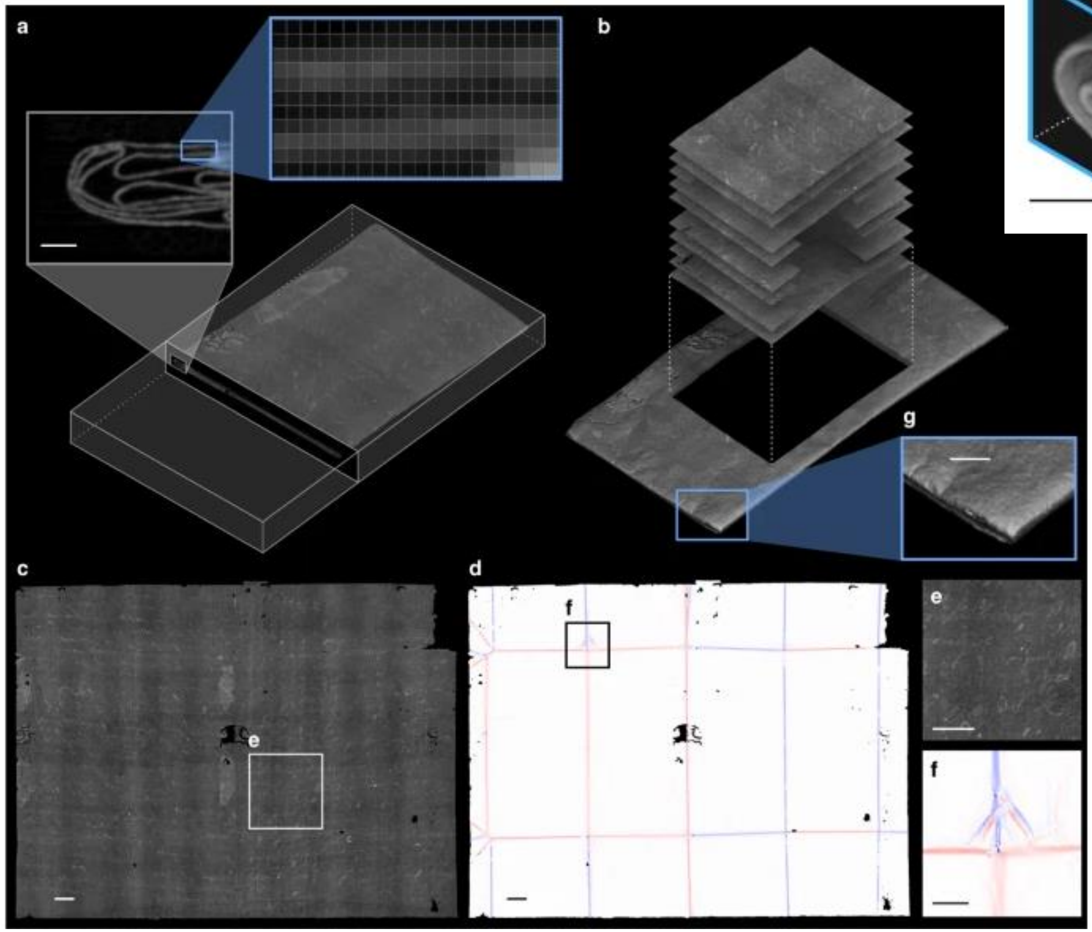

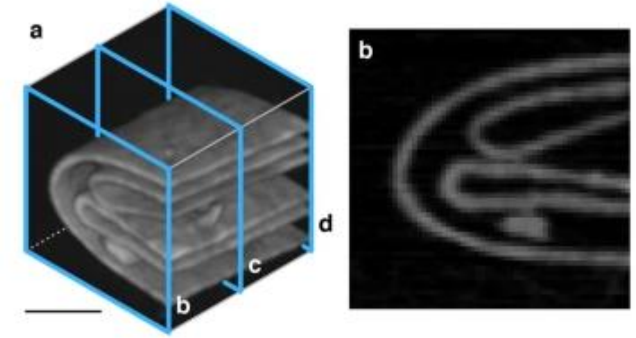

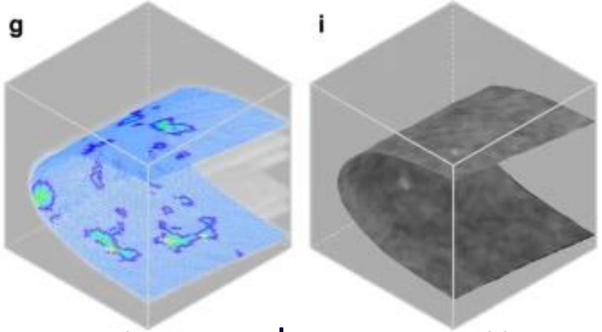

curvature and crease pattern

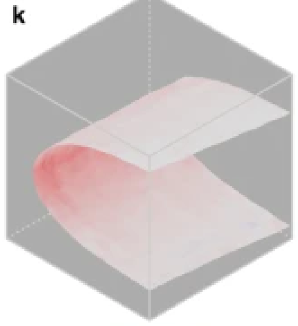

BEAmline for Tomography at SESAME

Funded by the EU's H2020 framework programme under grant agreement n°822535

Thank you for your attention

Further information

BEATS webpage: https://beats-sesame.eu

SESAME webpage: https://www.sesame.org.jo

Gianluca Iori: gianluca.iori@sesame.org.jo

BEATS_eu

@BEATSeu1

Bibliography:

1. Willmot P. An Introduction to Synchrotron Radiation: Techniques and Applications. John Wiley & Sons; 2019. 501 p.
2. A. Rack et al., Comparative study of multilayers used in monochromators for synchrotron-based coherent hard X-ray imaging, J Synchrotron Rad, vol. 17, no. 4, pp. 496–510, Jul. 2010.
3. A. Pogany, D. Gao, and S. W. Wilkins, “Contrast and resolution in imaging with a microfocus x-ray source,” Review of Scientific Instruments, vol. 68, no. 7, pp. 2774–2782, Jul. 1997.
4. Cloetens P. Phase Contrast Imaging - Coherent Beams [Internet]. School on X-ray Imaging Techniques at the ESRF; 2007 Feb 5 [cited 2020 Apr 21]; ESRF, Grenoble, France. link
5. C. Muñoz Pequeño, J. M. Clement, P. Thevenau, and P. Van Vaerenbergh, “Development of a Linear Fast Shutter for BM05 at ESRF and BEATS at SESAME,” presented at the MEDSI’20, Chicago, USA, Jul. 2021.
6. F. Mokoena, M. Bhamjee, P. Van Vaerenbergh, G. Iori, A. Kaprolat, and S. Connell, “An FEA Investigation of the Vibration Response of the BEATS Detector Stage,” presented at the MEDSI’20, Chicago, USA, Jul. 2021.
7. A. Mittone, I. Manakov, L. Broche, C. Jarnias, P. Coan, and A. Bravin, “Characterization of a sCMOS-based high-resolution imaging system,” Journal of Synchrotron Radiation, vol. 24, no. 6, pp. 1226–1236, 2017.
8. M. Rivers and F. De Carlo, “TomoScan 0.1” https://tomoscan.readthedocs.io/en/latest/about.html.
9. F. Bernardini et al., “Beeswax as Dental Filling on a Neolithic Human Tooth,” PLoS One, vol. 7, no. 9, Sep. 2012.
10. D. J. M. Ngan-Tillard, D. J. Huisman, F. Corbella, and A. Van Nass, “Over the rainbow? Micro-CT scanning to non-destructively study Roman and early medieval glass bead manufacture,” Journal of Archaeological Science, vol. 98, pp. 7–21, Oct. 2018.
11. S. Jahn and J. Klein, “Lubrication of articular cartilage,” Physics Today, vol. 71, no. 4, pp. 48–54, Apr. 2018.
12. Kersh ME. Resolving nanoscale strains in whole joints. Nat Biomed Eng. 2020 Mar;4(3):257–8.
13. Madi K, Staines KA, Bay BK, Javaheri B, Geng H, Bodey AJ, et al. In situ characterization of nanoscale strains in loaded whole joints via synchrotron X-ray tomography. Nat Biomed Eng. 2020 Mar;4(3):343–54.
14. “Why the fate of our planet’s environment depends on the state of its soil.”, 2021, https://theconversation.com/.
15. H. V. Cooper, S. Sjogersten, R. M. Lark, and S. J. Mooney, “To till or not to till in a temperate ecosystem? Implications for climate change mitigation,” Environ. Res. Lett., Feb. 2021.
16. A. C. Kaya, P. Zaslansky, A. Rack, S. F. Fischer, and C. Fleck, “Foams of Gray Cast Iron as Efficient Energy Absorption Structures: A Feasibility Study,” Advanced Engineering Materials, vol. 21, no. 6, p. 1900080, 2019.